

文章编号: 1671-1505(2025)03-0541-19 DOI: 10.7605/gdxb.2025.063

准噶尔盆地南缘晚侏罗世风成一冲积沉积特征 及古环境恢复*

关旭同¹ 王国荣² 孙 潇² 张亚楠¹
初亚男¹ 任楚楚¹ 吴朝东¹

1 北京大学造山带与地壳演化教育部重点实验室, 地球与空间科学学院, 北京 100871

2 核工业二一六大队, 新疆乌鲁木齐 830011

摘 要 中亚内陆地区晚侏罗世气候干旱化, 准噶尔盆地发育风成沉积, 该风成沉积的分布范围和共存的沉积体系还有待研究。为探究该问题, 作者对准噶尔盆地南缘上侏罗统进行了详细的沉积学考察, 发现喀拉扎组风成沉积位于侏罗系—白垩系不整合面之下, 沉积记录范围东西向可达 100 km, 最厚处约 250 m, 其中建功煤矿剖面的风成沉积砂体厚度十余米, 受到多期砾质辫状河的冲刷。风成沙具有较好的成分成熟度和结构成熟度, 以跳跃组分为主。风成沙丘具有大型高角度交错层理和反粒序层理, 风成沙席发育平行层理和低角度交错层理, 侧向延续性好。河流沙和同期的风成沙具有相似的粒度组成和沉积物源, 古风向与河流古流向正交, 这说明了风成物源来自于附近河流沙, 河流沙来自于风成沙地。晚侏罗世风成一冲积沉积体系受到气候干旱化和天山构造活动的控制, 气候干旱导致沉积物供给减少, 基准面下降, 辫状河转换为季节性曲流河; 天山的构造活化导致基准面下降, 在准噶尔盆地南缘风成沉积扩大, 且形成广泛分布的冲积扇砾岩。准噶尔盆地南缘侏罗纪至早白垩世沉积环境发生了从沼泽遍布的河流—三角洲体系演化到风成一冲积沉积体系、再到湖泊—三角洲沉积体系的 2 次重要变化, 记录了中亚地区晚侏罗世气候变干和早白垩世气候转为半湿润的气候变化, 可能与侏罗纪真极移事件和古天山水汽阻隔有关。

关键词 喀拉扎砾岩 侏罗系—白垩系不整合面 盆缘沉积 干旱环境 无人机建模 准噶尔盆地**第一作者简介** 关旭同, 男, 1996 年生, 博士后, 主要从事沉积学研究。E-mail: guanxt@pku.edu.cn。**通讯作者简介** 吴朝东, 男, 1965 年生, 教授, 博士生导师, 主要从事沉积学和储层地质学研究。E-mail: cdwu@pku.edu.cn。中图分类号: P512.2⁺1 文献标志码: A

Sedimentary characteristics of the Late Jurassic eolian and alluvial deposits in southern margin of Junggar Basin and palaeoenvironment reconstruction

GUAN Xutong¹ WANG Guorong² SUN Xiao² ZHANG Ya'nán¹
CHU Ya'nán¹ REN Chufan¹ WU Chaodong¹1 Key Laboratory of Orogenic Belts and Crustal Evolution, Ministry of Education, School of Earth and Space Sciences,
Peking University, Beijing 100871, China

2 Geologic Party No. 216, China National Nuclear Corporation, Urumqi 830011, China

* 新疆维吾尔自治区重大科技专项 (编号: 2024A03003) 资助。[Financially supported by Major Science and Technology Project of the Xinjiang Uygur Autonomous Region (No. 2024A03003)]

收稿日期: 2025-01-21 改回日期: 2025-02-13

Abstract The Late Jurassic climate in Central Asia was arid. The existence of the eolian deposits of the Junggar Basin in the southern Central Asia is contentious. In order for a better understanding of these eolian deposits, here we conducted detailed sedimentary investigations on the Upper Jurassic strata of the southern Junggar Basin. The eolian deposits of the Kalazha Formation underlie the Jurassic-Cretaceous unconformity. The sedimentary records extend ~100 km from east to west. The thickest eolian deposits are ~250 m in thickness. The Jiangong mine section exhibits approximately 10-meter-thick eolian deposits and several stages of gravely braided river deposits. The eolian sands show high compositional and textural maturity and are mainly composed of saltation grains. The eolian dune deposits show large-scale, high-angle cross-bedding and inverse-grading. The eolian sheet deposits develop low-angle oblique and parallel laminations with good lateral continuity. The river sands and coeval eolian sands have similar grain-size distribution and sediment sources. The paleo-wind direction is orthogonal to the river flow direction. These suggest that the eolian sands were sourced from river sands and the river sands were partly from the eolian dune field. The eolian-fluvial system was controlled by the Late Jurassic aridification and tectonic activities of the Tianshan orogen. The aridity caused the decrease of sediment supply and the rise of the base level, which caused the expansion of the eolian deposits. The tectonic reactivation of the Tianshan led to dropping of the base level, the formation of Kalazha alluvial conglomerates. The Jurassic to the Early Cretaceous sedimentary environments of the southern Junggar Basin witnessed two important changes: the marshy fluvial-lacustrine sedimentary system changed to eolian-alluvial system, and subsequently evolved to lacustrine-delta system. These climatic changes may be related to the Jurassic true polar wander and block of the moisture by the paleo-Tianshan.

Key words Kalazha conglomerate, Jurassic-Cretaceous unconformity, basin margin sedimentation, arid environment, unmanned aerial vehicle modeling, Junggar Basin

About the first author GUAN Xutong, born in 1996, postdoctoral position, is mainly engaged in sedimentary geology. E-mail: guanxt@pku.edu.cn.

About the corresponding author WU Chaodong, born in 1965, is a professor and Ph.D. supervisor of Peking University. He is mainly engaged in sedimentology and reservoir geology. E-mail: cdwu@pku.edu.cn.

0 引言

中亚和东亚的很多地区在晚中生代发生干旱化 (Yi *et al.*, 2019)。晚侏罗世旱生植物广布 (Zhang *et al.*, 2014; 邓胜徽等, 2015; Xie *et al.*, 2024), 准噶尔盆地南缘 (Fang *et al.*, 2016; Jolivet *et al.*, 2017; Morin *et al.*, 2018; Guan *et al.*, 2024)、宁武—静乐盆地 (Xu *et al.*, 2019) 和蒙阴盆地 (许欢等, 2013) 发育风成沉积。早白垩世众多盆地形成了广泛的风成沉积 (许欢等, 2013), 如准噶尔盆地西北缘 (Guan *et al.*, 2024) 和东北缘 (Eberth *et al.*, 2001; Vincent and Allen, 2001; Xu *et al.*, 2022)、吐哈盆地 (Zhang *et al.*, 2025)、库车盆地 (梅冥相等, 2004)、柴达木盆地 (胡俊杰等, 2018; 陈政宇等, 2020)、塔里木盆地西南

缘 (陈荣林等, 1994)、民乐—张掖盆地 (梅冥相和苏德辰, 2014a)、兰州盆地 (梅冥相和苏德辰, 2014b) 和白银—靖远盆地 (Wang *et al.*, 2024), 鄂尔多斯盆地则发育沙漠沉积 (李孝泽等, 1999; Qiao *et al.*, 2022)。位于中亚地区的准噶尔盆地受到中侏罗世晚期开始的干旱化的影响, 煤层消失, 出现石膏薄层, 旱生植物孢子 *Classopollis* 大量增加, 直至成为孢粉组合的主要组分 (邓胜徽等, 2015), 湖泊萎缩, 发育季节性曲流河、浅水三角洲、红色冲积扇砾岩和风成沉积 (高志勇等, 2015; Fang *et al.*, 2016; Jolivet *et al.*, 2017; Morin *et al.*, 2018; 关旭同等, 2019; 张驰等, 2021; Gao *et al.*, 2022; 张昌民等, 2023; Guan *et al.*, 2024)。

在干旱气候下, 准噶尔盆地发育风成沉积。

Fang 等 (2016) 发现风成沉积夹层出现在上侏罗统齐古组河流相地层中, Jolivet 等 (2017) 在准噶尔盆地南缘头屯河剖面报道了上侏罗统喀拉扎组的风成沉积, Guan 等 (2022, 2024) 对这一区域的喀拉扎组风成砂岩进行了系统研究和沉积对比, Morin 等 (2018) 通过沉积对比重建了晚侏罗世—早白垩世准噶尔盆地古地理, 认为从古天山山前至卡拉麦里山前风成沉积广布; 一些学者提出喀拉扎组还发育季节性辫状河 (高志勇等, 2015)、辫状河三角洲前缘河道 (司学强等, 2021) 或辫状河三角洲前缘河口坝沉积 (Schneider *et al.*, 1992)。

为探究风成沉积的分布范围和共存的沉积体系并重建准噶尔盆地南缘晚侏罗世—早白垩世沉积环境, 对准噶尔盆地南缘上侏罗统露头进行了沉积学分析, 认为上侏罗统喀拉扎组发育风成沉积, 并建立了风成—冲积体系的沉积模式, 然后探讨了中亚晚侏罗世古环境和古气候。

1 地质背景

准噶尔盆地位于中亚造山带的南部, 自中生代以来, 被天山、西准噶尔、东准噶尔和阿尔泰造山带所包围 (图 1-a)。在经历了古生代的岛弧和陆块的拼合后, 准噶尔盆地在早二叠世成为裂谷盆地 (方世虎等, 2006; Wang *et al.*, 2018), 在三叠纪至中侏罗世早期为断—拗盆地 (张朝军等, 2006; 何登发等, 2018; Wang *et al.*, 2018), 在南缘的局部地区可识别出三叠纪—侏罗纪地垒和地堑 (Guan *et al.*, 2016; Wang *et al.*, 2018; 梁则亮等, 2020)。从中侏罗世晚期到晚侏罗世为压扭盆地 (何登发等, 2018; Peng *et al.*, 2024), 早白垩世为拗陷盆地, 到晚白垩世构造背景转为挤压 (Wang *et al.*, 2018)。

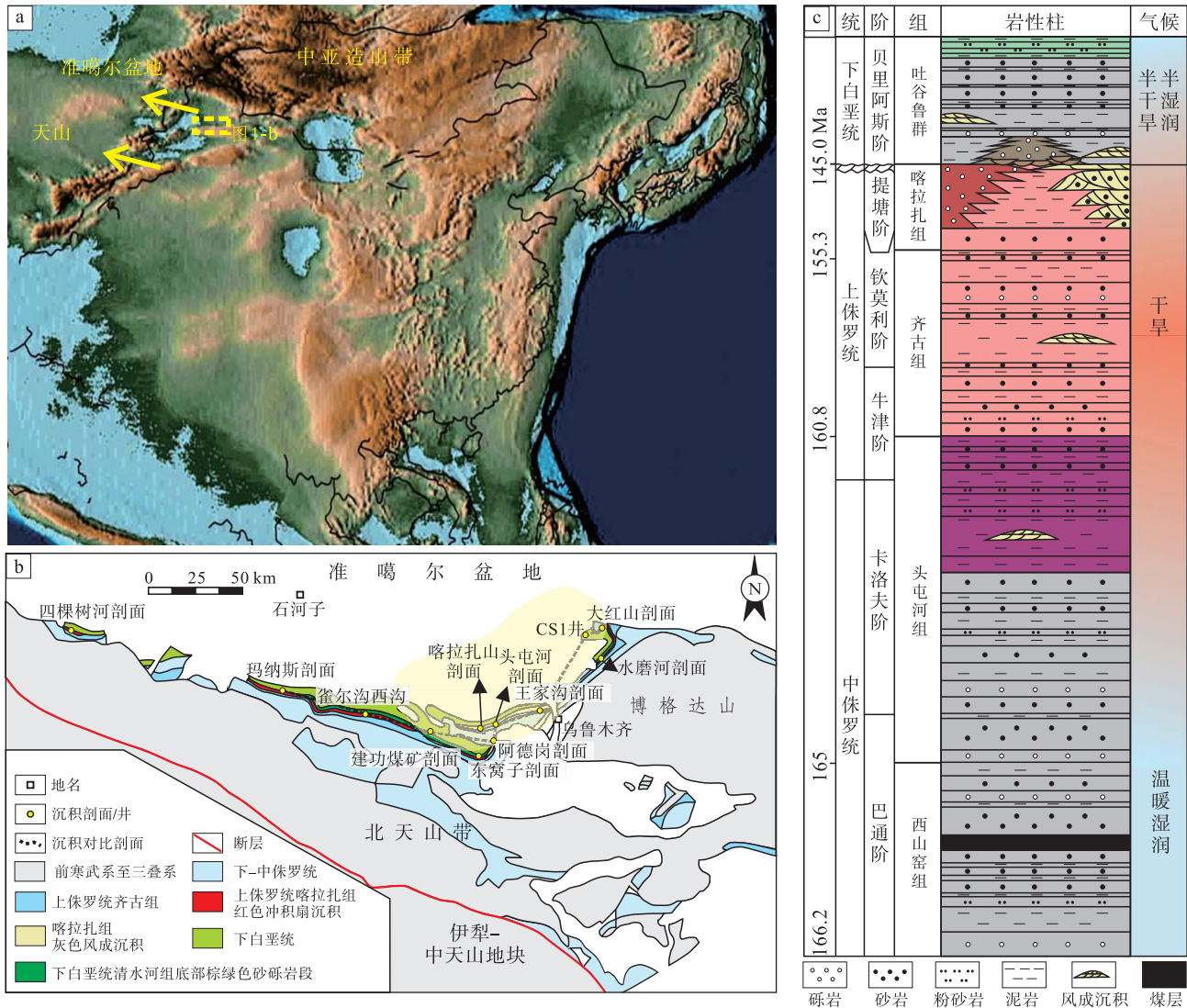
准噶尔盆地南缘侏罗系包括下侏罗统八道湾组和三工河组、中侏罗统西山窑组和头屯河组以及上侏罗统齐古组和喀拉扎组。八道湾组岩性为灰色砂岩、泥岩、碳质泥岩及煤层, 三工河组岩性为黄色砂岩和灰绿色、灰黑色泥质粉砂岩、粉砂岩和泥岩; 西山窑组岩性为灰色砂岩和泥岩, 含煤层; 头屯河组下部以灰绿色砂岩和泥岩为主, 上部以紫红色砂岩和泥岩为主; 齐古组的岩性为红色砂岩和泥岩; 喀拉扎组岩性包括红色、褐绿色厚层砾岩和灰色厚层砂岩。下白垩统吐谷鲁群自下而上包括清水

河组、呼图壁组、胜金口组和连木沁组, 清水河组主要由灰绿色泥岩和砂岩组成, 夹紫红色砂质泥岩条带; 呼图壁组岩性为紫红色泥岩、泥质粉砂岩和粉砂岩, 夹灰绿色薄层砂岩、石灰岩; 胜金口组岩性为绿色泥岩和粉砂岩; 连木沁组岩性为褐红、灰绿色泥岩和灰绿色砂岩 (新疆维吾尔自治区地质矿产局, 1999)。侏罗系与白垩系之间存在角度不整合, 可见于齐古背斜剖面 and 地震剖面 (Fang *et al.*, 2016; Jolivet *et al.*, 2017)。

早侏罗世至中侏罗世早期, 准噶尔盆地及邻近盆地气候温暖湿润 (Wang *et al.*, 2005; Ashraf *et al.*, 2010; Sha *et al.*, 2015, 2023; 田业, 2017; Morin *et al.*, 2018), 发育煤层和丰富的植物化石 (Sha *et al.*, 2015)。从中侏罗世巴通期开始, 准噶尔盆地及邻近盆地的孢粉记录证明气候转变为季节性干旱 (Wang *et al.*, 2005; Ashraf *et al.*, 2010; Jolivet *et al.*, 2017; Morin *et al.*, 2018), 指示干旱气候的孢子 *Classopollis* 明显增加 (邓胜徽等, 2015)。在准噶尔盆地地层中发育指示蒸发、干旱气候的薄层石膏 (Fang *et al.*, 2016)、钙质古土壤和风成沉积 (Jolivet *et al.*, 2017)。早白垩世, 准噶尔盆地及邻近盆地的孢粉组合指示古气候比晚侏罗世有所湿润 (王长轩, 2014; Zhang *et al.*, 2014; 邓胜徽等, 2015), 为季节性干旱 (Eberth *et al.*, 2001)。

2 研究方法

重点选取准噶尔盆地南缘建功煤矿 (86°42' 27.86" E, 43°47'17.68"N) 和喀拉扎山剖面 (87°10'17.76"E, 43°46'12.33"N) 进行沉积学分析, 并对比了玛纳斯、阿德岗、头屯河、王家沟和大红山剖面以及 CS1 井。风成沉积的沉积构型规模较大, 近处观察难以看到全貌, 因此借助无人机拍照、建模进行全面的观察并识别沉积界面、沉积构造、构型等 (Nieminski and Graham, 2017)。无人机在多个距离捕获建功煤矿和喀拉扎山剖面数百张高分辨率 (2000 万像素) 的图像。照片采用倾斜和平行角度拍摄, 三维空间重叠度不低于 75%, 以确保后期处理的高精度 (Westoby *et al.*, 2012; Chesley *et al.*, 2017)。无人机型号为 DJI Matrice 350 RTK, 建模采用大疆智图软件。



为清楚展示地层展布，图中的上侏罗统一下白垩统分布范围稍有夸大

图 1 晚侏罗世亚洲古地理图 (a; Scotese, 2016)、准噶尔盆地南缘上侏罗统一下白垩统地层分布 (b) 和地层综合柱状图 (c; Guan *et al.*, 2024)

Fig. 1 Late Jurassic palaeogeographic map of Asia (a; Scotese, 2016), stratigraphic distribution (b), and comprehensive stratigraphic column (c; Guan *et al.*, 2024) of the Upper Jurassic and Lower Cretaceous in southern margin of Junggar Basin

3 沉积相分析

通过对准噶尔盆地南缘的建功煤矿、喀拉扎山、玛纳斯、阿德岗、头屯河、王家沟和大红山剖面以及 CS1 井的沉积学分析(图 2)，把 11 类岩相划分为 3 种岩相组合(表 1; 图 2)，解释为冲积扇、风成沉积和河流沉积相(表 2)。

3.1 风成砂丘

岩相组合 1.1 发育在上侏罗统齐古组和喀拉扎组(表 2)，发育 Sgf 和 Sh 这 2 种岩相。结合野外

地质观察和无人机建模，识别了以风成叠合面、风成再作用面、丘间迁移面为界面的风成沙丘、沙席和丘间沉积(图 3; Mountney, 2006)，风成前积层的风成叠合面指示了叠合的类新月形沙丘顺风向的迁移 (Rodríguez-López *et al.*, 2008)。喀拉扎组的该岩相组合位于侏罗系—白垩系不整合面之下(图 2; 图 4)。

喀拉扎组发育大型槽状或板状高角度交错层理(图 5-a, 5-c, 5-d)。喀拉扎组大型交错层理厚度为 3~5 m，校正后的交错层理角度范围为 12.1°

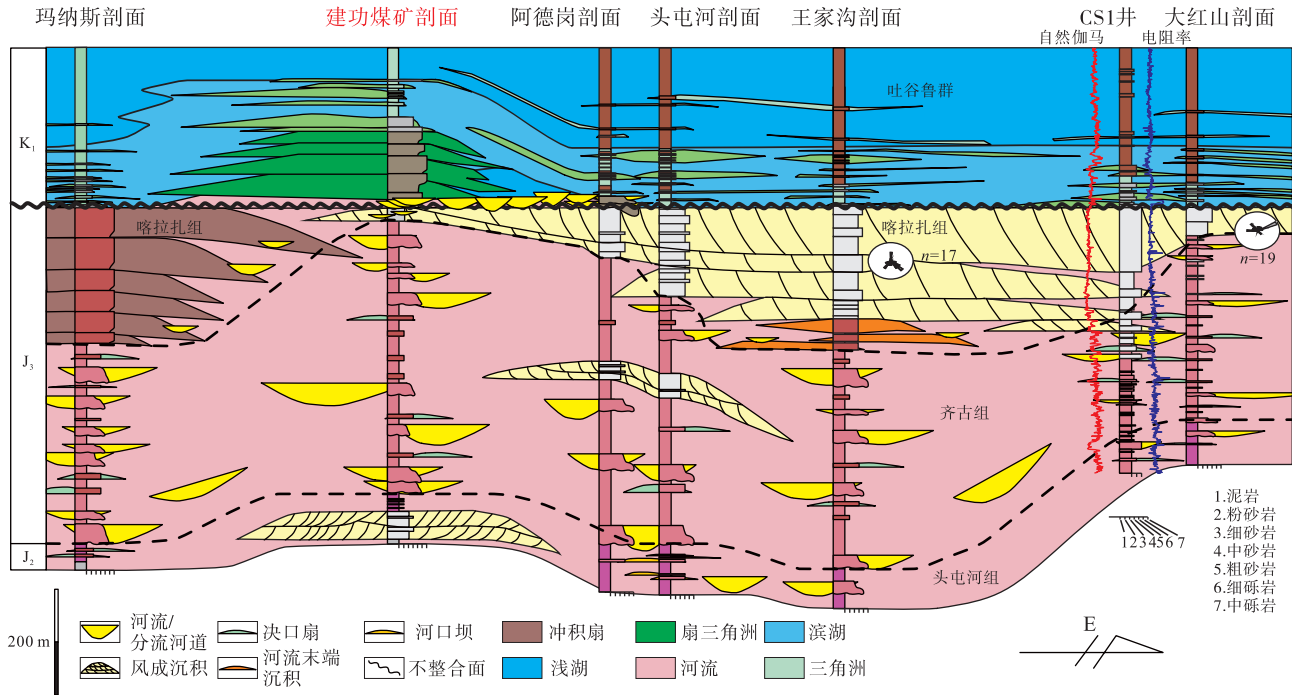


图 2 准噶尔盆地南缘上侏罗统一下白垩统沉积对比 (修改自 Guan *et al.*, 2024)

Fig. 2 Sedimentary correlation of the Upper Jurassic and Lower Cretaceous in southern margin of Junggar Basin (modified from Guan *et al.*, 2024)

表 1 准噶尔盆地南缘上侏罗统一下白垩统沉积相

Table 1 Sedimentary facies of the Upper Jurassic to Lower Cretaceous of southern margin of Junggar Basin

岩相代码	岩性	沉积结构及沉积构造	沉积机理分析
砾岩岩相	Gmm 数十米厚细砾岩至中砾岩	杂基支撑,块状构造,喀拉扎组中见震积构造	快速沉积
	Gcm 数分米至数米厚细砾岩	颗粒支撑,部分发育交错层理,部分为块状构造,发育砾石叠瓦状或水平排列	牵引流或受潮流改造
砂岩岩相	Sr 数厘米至数分米厚细砂岩或粉砂岩	浪成或者流水波痕和沙纹层理	波成或流水波痕迁移
	Sc 数厘米至数分米厚细砂岩或中砂岩	变形层理,部分为包卷层理	水塑性 (hydroplastic) 或液化变形
	Sm 数厘米厚中砂岩或粗砂岩	块状构造	快速沉积
	Sh 数厘米至数分米厚中砂岩或粗砂岩	平行层理和流水线理	具有上部流动机制的牵引流
	Sp 数分米厚细砂岩至粗砂岩	板状交错层理	二维床砂底形 (bedform) 迁移
	St 数分米厚中砂岩至粗砂岩	槽状交错层理	三维床砂底形 (沙丘) 迁移
	Sgf 数米至数十米厚中砂岩至粗砂岩	数米厚高角度交错层理	风成波痕迁移和边界流分离带中颗粒飘落的产物
泥岩和粉砂岩岩相	Fsm 数厘米至数分米厚的细砂岩、粉砂岩或泥岩	泥裂、钙质结核、生物扰动 (<i>Scoyenia</i> 遗迹相)	悬浮沉积,伴随暴露事件
	Fl 数厘米至数分米厚的细砂岩、粉砂岩或泥岩	水平层理,薄层泥岩、粉砂岩、细砂岩和石膏互层沉积	静水悬浮沉降,交替有溢岸沉积、蒸发盐沉积

~36.1° (Guan *et al.*, 2024)。部分交错层理砂岩中可以观察到氧化的黄铁矿,可观察到反粒序层理 (图 5-b),由分选和磨圆良好到中等的次棱角状到次圆状中一细砂岩组成 (图 6),以跳跃组分为主

(图 7-a; Guan *et al.*, 2024)。砂岩颗粒表面呈现碟形、新月形撞击坑 (图 6-f)。

该岩相组合解释为风成沙丘沉积。中一细粒砂为常见的风力搬运粒度,搬运方式以跳跃为主,具

表 2 准噶尔盆地南缘上侏罗统一白垩统主要岩相组合及沉积相解释

Table 2 Primary lithofacies association and interpretation of sedimentary facies of the Upper Jurassic to Lower Cretaceous of southern margin of Junggar Basin

岩相组合	地层	沉积构型	沉积相解释
岩相组合 1.1 —Sgf, Sh		高角度槽状和板状交错层理(图 5-a, 5-c, 5-d); 反粒序层理(图 5-b); 具有好、中等分选的次棱角状至次圆状的中、细砂岩(图 7-a, 7-b); 碟形、新月形撞击坑(Guan <i>et al.</i> , 2024); 以跳跃颗粒为主(图 7-a)	风成沙丘。具有颗粒流(grainflow)层和颗粒飘落(grainfall)层(Hunter, 1977; Mountney, 2006)
岩相组合 1.2 —Sc, Fsm, Fl	上侏罗统齐古组和喀拉扎组	<i>Scoyenia</i> 遗迹化石(Guan <i>et al.</i> , 2024)、泥裂(图 5-e)	丘间沉积。间发性暴露出水面(Frey <i>et al.</i> , 1984; Buatois and Mángano, 2004)
岩相组合 1.3 —Sh, Sr		分选好的次棱角状至次圆状的细砂岩(Guan <i>et al.</i> , 2024); 平行或低角度层理(图 3; 图 5-g); 厚度为 10~100 m(图 3-c, 3-f), 侧向延伸超过 1500 m(图 3-f); 风成波痕(Guan <i>et al.</i> , 2024)	风成沙席。具有平移层理(translatent strata; Hunter, 1977; Fryberger <i>et al.</i> , 1979; Kocurek and Dott, 1981)
岩相组合 2 —Gcm, Sp, St, Sr, Fsm	上侏罗统齐古组、喀拉扎组和下白垩统清水河组	数米厚的透镜状、板状或带状的砂体(图 4; 图 5; 图 8), 沉积序列一般由 Sp, St, Sr 和 Fsm 组成, 在部分沉积序列底部发育 Gcm, 砂岩颗粒具有中等分选、棱角状至次圆状的特点(图 6-c, 6-d, 6-f), 包括跳跃和滚动组分(图 7-b)	河流。砂体底部的颗粒支撑砾岩(Gcm)为河道底部滞留沉积(Allen, 1965; Hein and Walker, 1977)
岩相组合 3 —Gmm, Gcm, Sm, Sp, St	上侏罗统喀拉扎组	数十米厚的 Gmm 和数米厚的 Sm, 也可见一些 Gcm, Sp 和 St(图 9)	冲积扇。包括泥石流沉积、片流沉积和河道沉积(Nemec and Steel, 1984; Blair and McPherson, 1994)

有风力输送过程中的高速撞击造成的月牙形和碟形撞击坑, 这些特点都指示了典型的风成沙丘沉积(Xu *et al.*, 2019)。大规模的高角度交错层理是风成波痕迁移和边界流分离带中颗粒飘落的产物(图 5-a, 5-c, 5-d; Hunter 1977; Clemmensen and Abrahamsen, 1983)。反粒序层理为颗粒流沉积(图 5-b), 发生在沿风成沙丘背风坡的颗粒流崩塌中(Hunter, 1977; Mountney, 2006), 粒度相对较细的水平层理是颗粒飘落的结果。风成沙丘沉积中经常发生侵蚀(Elbelrhiti *et al.*, 2008), 表现为风成再作用面和叠合面(图 3-c, 3-f; Kocurek, 1991)。准噶尔盆地南缘的晚侏罗世和早白垩世的河流、冲积扇沉积的古流向普遍为自南向北(Fang *et al.*, 2016; 周天琪等, 2019; Guan *et al.*, 2022), 而通过测量晚侏罗世风成沉积的大型高角度交错层理的产状并校正得到的古风向为自西向东(图 2)。

3.2 风成沙席和丘间沉积

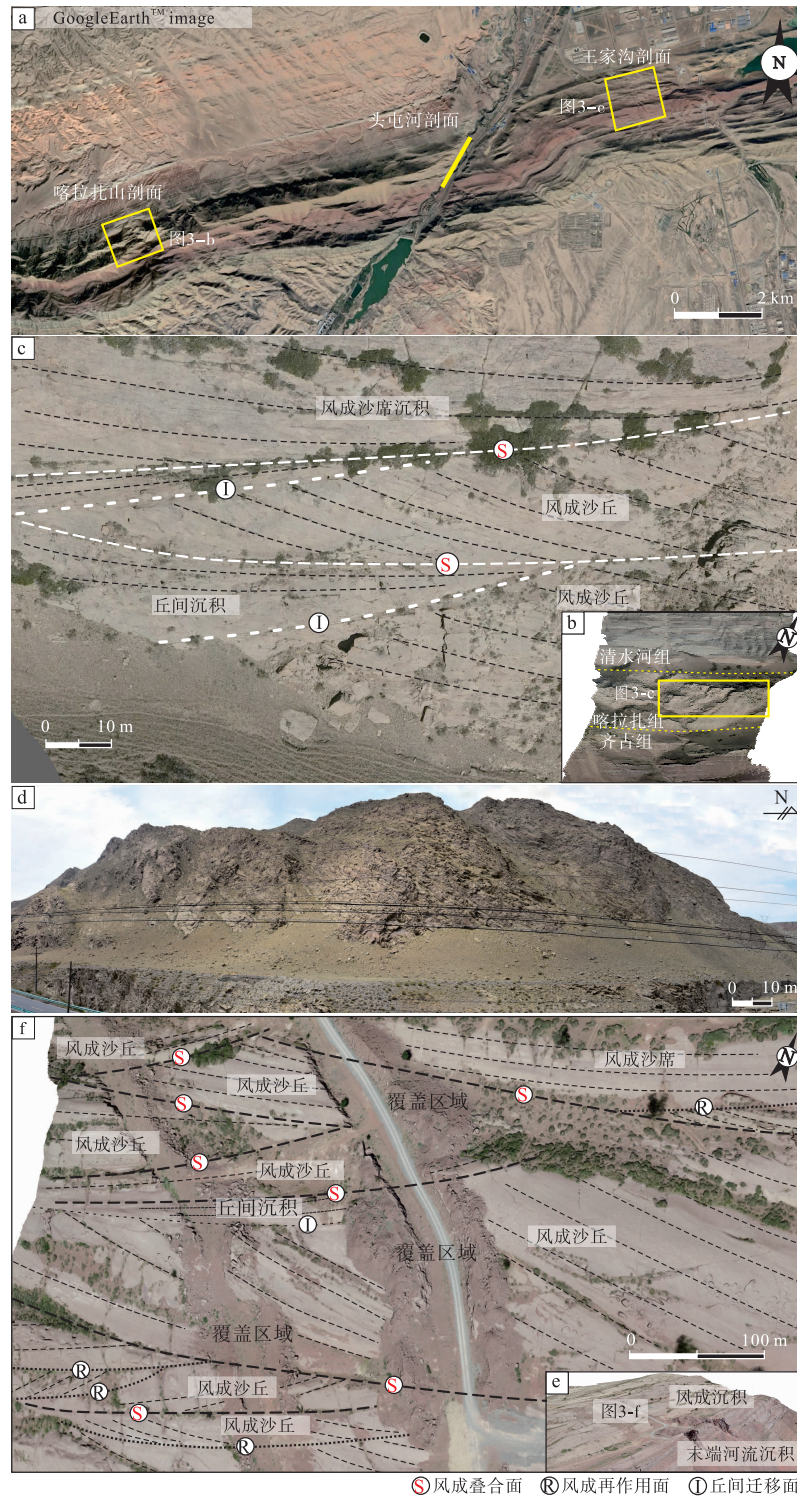
岩相组合 1.2 由 Sc、Fsm 和 Fl 岩相组成, 在王家沟剖面的喀拉扎组中厚度达数分米, 可见 *Scoyenia* 遗迹化石(Guan *et al.*, 2024), 在建功煤矿剖面发育泥裂(图 5-e)。泥裂和丘间的 *Scoyenia* 遗迹化石都表明间发性暴露出水面的环境(Frey

et al., 1984; Buatois and Mángano, 2004), 该岩相组合解释为丘间沉积。

岩相组合 1.3 由 Sh 和 Sr 岩相组成, 发育于大红山剖面的喀拉扎组下部、王家沟和喀拉扎山剖面的喀拉扎组上部(图 3-c, 3-f), 岩性为分选性较好、形状呈次棱角状至次圆状的细砂岩, 可见平行层理和低角度层理, 具有反粒序, 发育风成波痕, 具有波脊粒度较粗的特点(Guan *et al.*, 2024)。砂体垂向厚度达 10~100 m, 侧向延伸性好, 超过 1500 m(图 3)。该岩相组合分别解释为风成沙席沉积。风成沙席具有横向连续性好的特点, 发育平行或低角度层理, 层理具有反粒序, 是由平移层理(translatent strata)造成(Hunter, 1977; Fryberger *et al.*, 1979; Kocurek and Dott, 1981; Mountney, 2006; Simplicio and Basilici, 2015; Cao *et al.*, 2023)。风成沙丘、沙席和丘间沉积交替出现, 以水平的风成再作用面为界(Mountney, 2006; 图 3-c, 3-f)。

3.3 河流沉积

岩相组合 2 分布于上侏罗统齐古组、喀拉扎组和下白垩统清水河组, 在建功煤矿剖面的喀拉扎组中岩相组合 2 和岩相组合 3 互层, 由 Gcm, Sp, St, Sr, Fsm 岩相组成(表 2), 齐古组可见钙质古



a—来自 GoogleEarth™ 软件的卫星图像；b—喀拉扎山剖面无人机建模区域（87°10'17.76"E，43°46'12.33"N）；c—喀拉扎山剖面风成沉积砂体构型；d—头屯河剖面风成沉积（87°15'38.88"E，43°47'2.24"N）；e—王家沟剖面无人机建模区域（87°19'4.43"E，43°47'53.04"N），模型可在 DDE outcrop3D 网站上查看（SFT01-Wangjiagou）：<https://outcrop3d.deep-time.org/?model=62f81418-7121-901c-6736-412354b137c6>；f—王家沟剖面风成沉积砂体构型；风成沉积的界面识别采用 Mountney（2006）的方案，包括风成叠加面（S）、风成再作用面和风成沙丘间迁移面（I）（Guan *et al.*，2024）

图 3 准噶尔盆地南缘上侏罗统喀拉扎组典型风成沉积

Fig. 3 Typical eolian deposits of the Upper Jurassic Kalazha Formation in southern margin of Junggar Basin

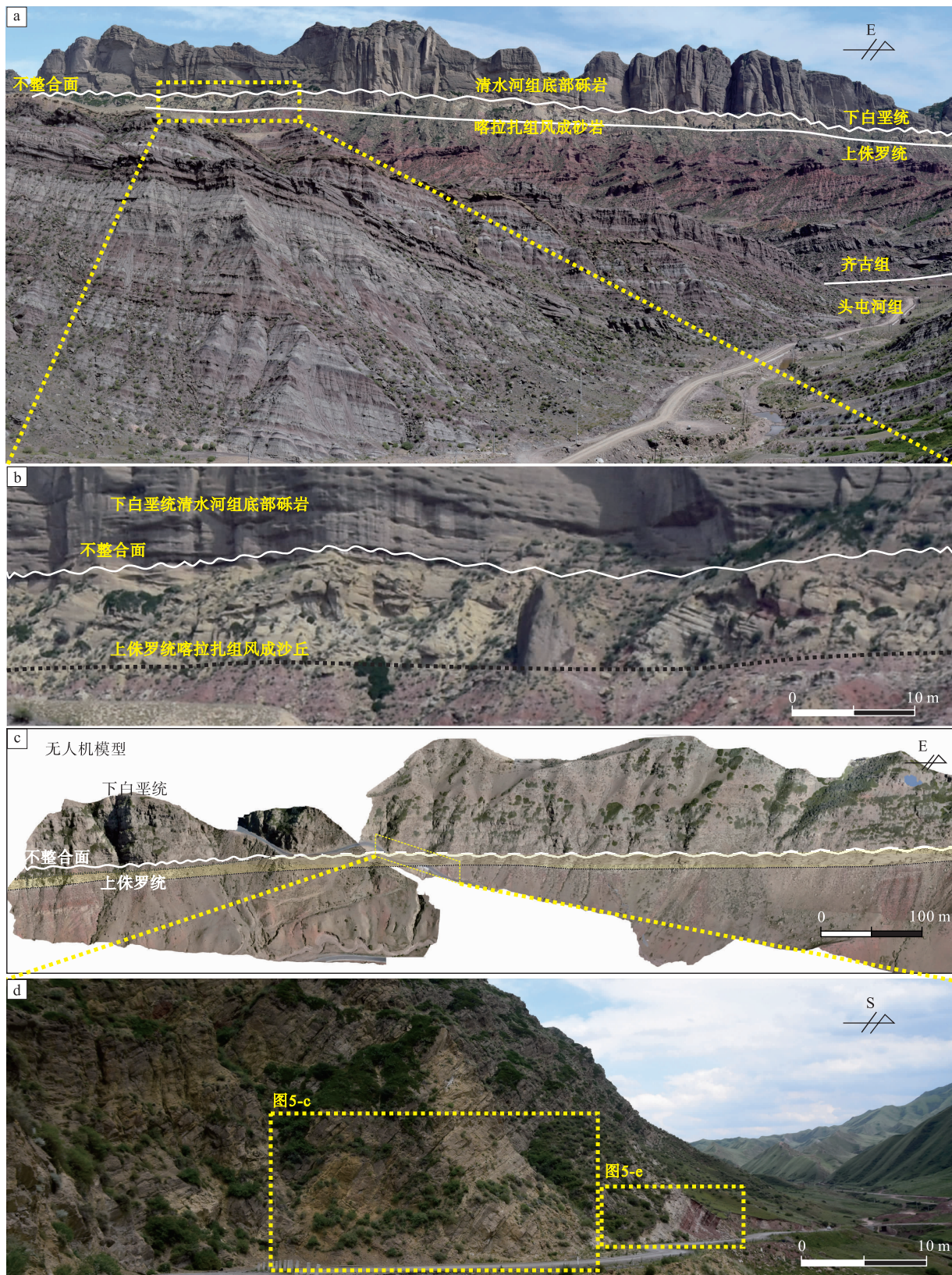
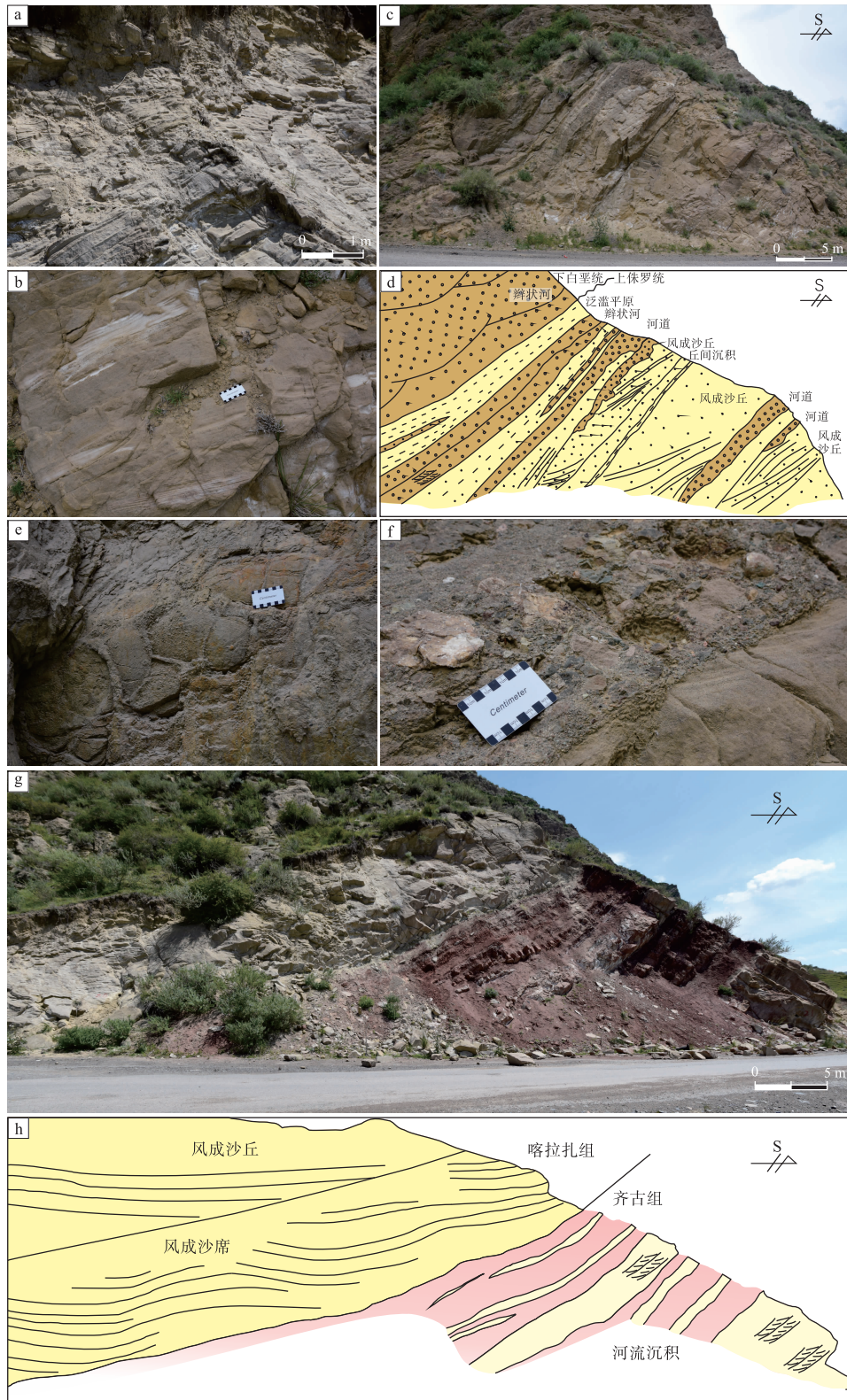
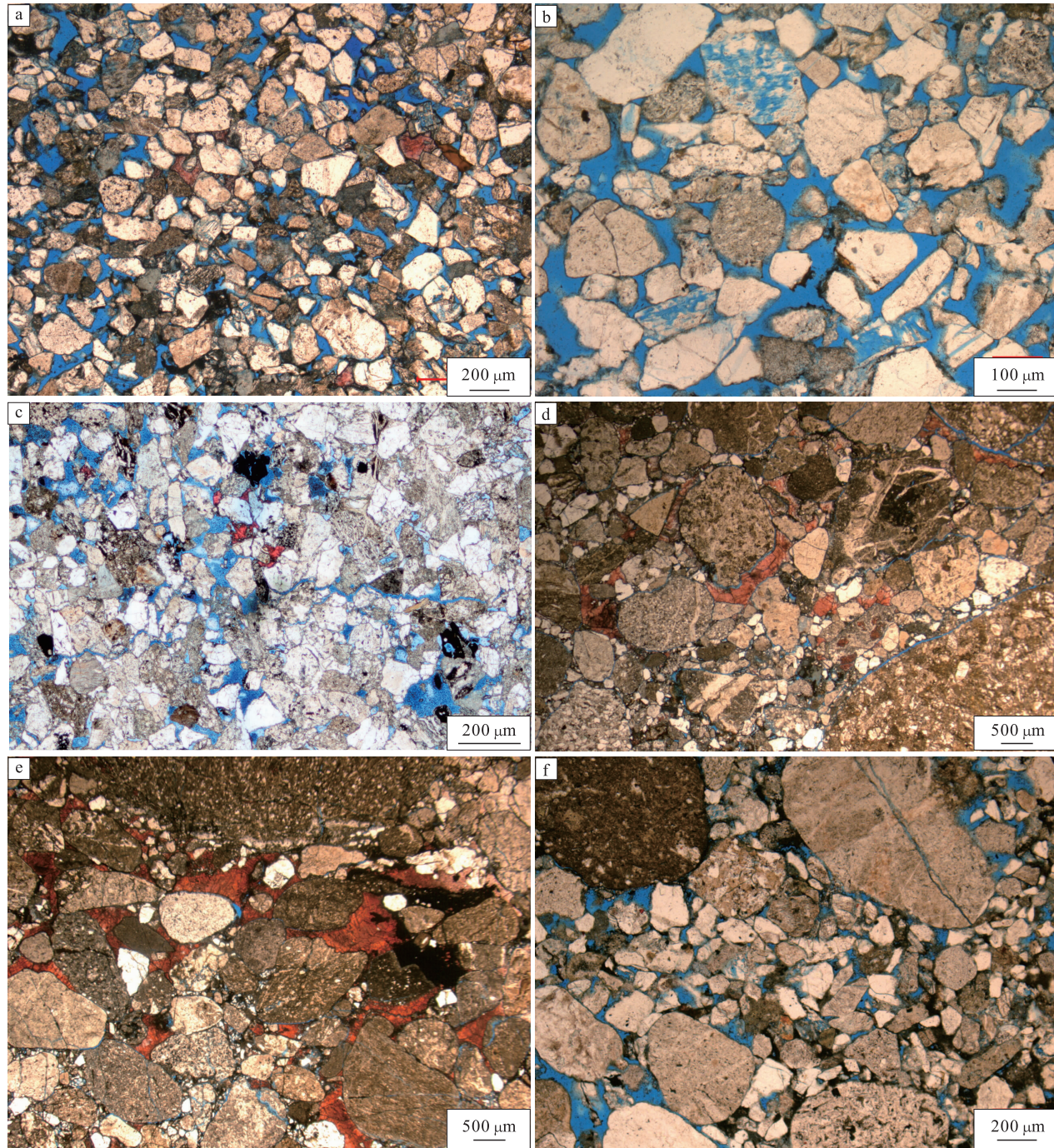


图 4 准噶尔盆地南缘建功煤矿剖面侏罗系—白垩系不整合面和上侏罗统喀拉扎组风成沉积
 Fig. 4 Jurassic-Cretaceous unconformity and the Upper Jurassic Kalazha Formation eolian deposits
 in Jiangong mine section of southern margin of Junggar Basin



a—大型风成高角度交错层理；b—反粒序层理和颗粒流沉积；c、d—辫状河和风成沉积互层；e—泥裂，丘间沉积；f—叠瓦状河流砾岩冲刷大型高角度交错层理风成砂岩；g、h—喀拉扎组风成沉积上覆齐古组曲流河沉积

图 5 准噶尔盆地南缘建功煤矿剖面上侏罗统喀拉扎组风成沉积和河流沉积
 Fig. 5 Meandering river and eolian deposits of the Upper Jurassic Kalazha Formation
 in Jiangong mine section of southern margin of Junggar Basin



a—风成沉积，上侏罗统喀拉扎组，建功煤矿剖面；b—曲流河沉积，分选较好，上侏罗统齐古组，建功煤矿剖面；c—曲流河沉积，分选一般，上侏罗统齐古组，建功煤矿剖面；d—扇三角洲沉积，下白垩统清水河组，建功煤矿剖面；e—辫状河沉积，上侏罗统喀拉扎组，建功煤矿剖面；f—碟形坑和新月形坑，头屯河剖面（Guan *et al.*, 2024）。蓝色环氧树脂胶充填孔隙，茜素红 S 染料染色方解石为红色

图 6 准噶尔盆地南缘上侏罗统一下白垩统砂岩显微照片

Fig. 6 Microphotographs of the Upper Jurassic and Lower Cretaceous sandstones in southern margin of Junggar Basin

土壤 (Jolivet *et al.*, 2017)。具有底部冲刷面的透镜状或带状砂体发育在块状泥岩 (Fsm) 中，砂体由交错层理砂岩 (Sp、St) (图 8-e, 8-f) 和沙纹层理砂岩 (Sr) 组成，部分砂体底部可见颗粒支

撑砾岩 (Gcm) 或交错层理砾岩，可见叠瓦状砾石 (图 5-f; 图 8-a, 8-b)，整体构成正粒序，解释为河道或点坝沉积。部分地层序列为反粒序，层厚向上增加，可见沙纹层理和水平层理 (图 8-d)，

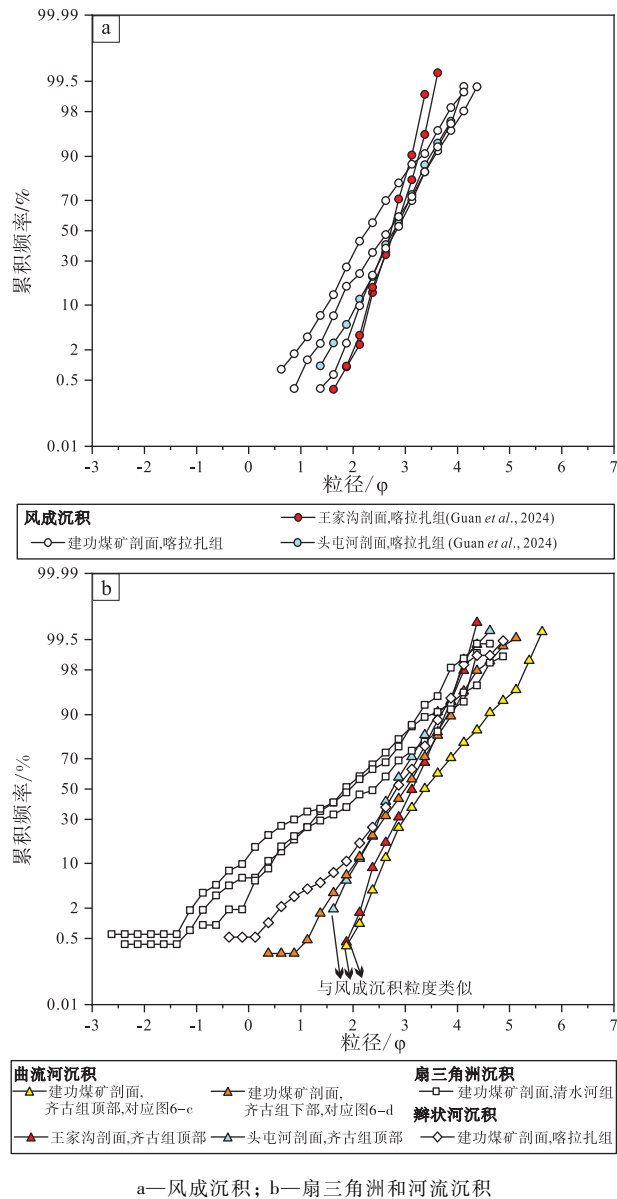


图 7 准噶尔盆地南缘上侏罗统粒度概率累积曲线
Fig. 7 Log-probability grain-size distribution curves of aeolian deposits in the Upper Jurassic of southern margin of Junggar Basin

解释为决口扇沉积。

在建功煤矿剖面，侏罗系—白垩系不整合面之下为喀拉扎组辫状河沉积与风成沉积互层(图 5-c, 5-d; 图 8-a)，不整合面之上为下白垩统清水河组频繁冲刷、多层叠置的辫状河厚层砂体(图 8-c)。河流沉积与下伏风成沉积之间的界面为洪泛面(图 5-c, 5-d, 5-f; 图 8-a; Langford and Chan, 1989)，风成沉积与下伏辫状河沉积的平直界面为风蚀丘间迁移面(图 8-a)。

在建功煤矿剖面，中侏罗统头屯河组上部上和上

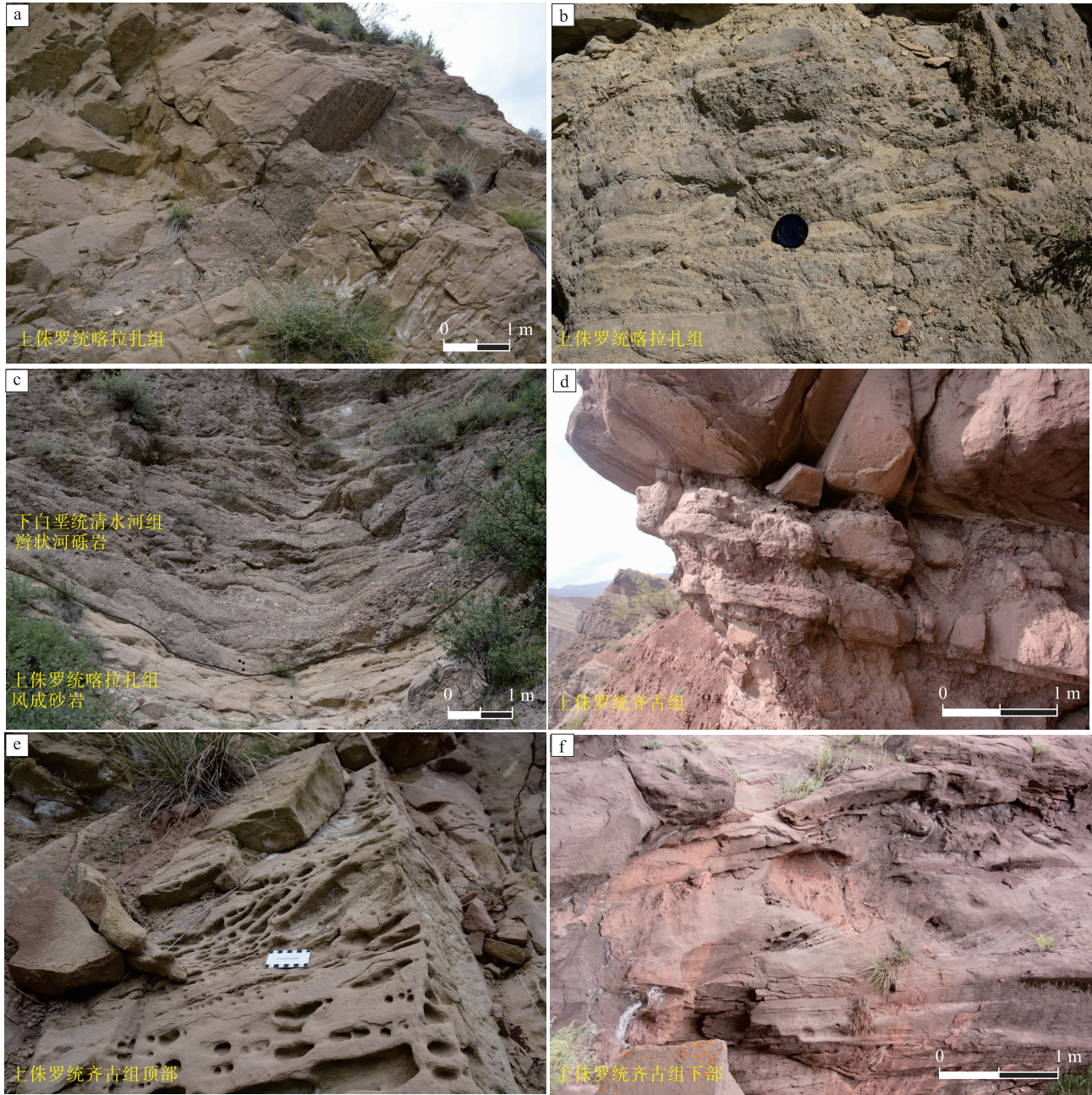
侏罗统齐古组砂体呈透镜状或带状发育于厚层泥岩中，可解释为曲流河沉积(Fang *et al.*, 2016; 关旭同等, 2019, 2020; Guan *et al.*, 2021, 2022)。齐古组下部的小型槽状交错层理曲流河砂岩为红色岩屑砂岩，分选、磨圆差(图 6-c; 图 8-f)，而齐古组顶部小型槽状交错层理曲流河砂岩为黄白色岩屑砂岩(图 6-d; 图 8-e)，颗粒磨圆好于前者，镜下特征和粒度概率累计曲线都与风成砂类似(图 6-a, 6-b, 6-c; 图 7)，王家沟和头屯河剖面的齐古组顶部的曲流河砂岩也具有类似的特点(图 7-b)，这是因为该河流砂经过了风力作用的搬运、分选和磨圆，具有了较高的结构成熟度。

3.4 冲积扇沉积

岩相组合 3 主要发育在上侏罗统喀拉扎组，在准噶尔盆地南缘广泛分布，包括了 Gmm、Gcm、Sm、Sp 和 St 这 5 种岩相(表 2)。在玛纳斯剖面可见互层的杂基支撑砾岩层与块状的砂岩层(图 9-c)和具有底部冲刷面的砂砾岩透镜体(图 9-d)，分别为冲积扇的片流和河道沉积。在四棵树河剖面，喀拉扎组下部的砾岩具有无分选和砾石棱角状的特点，而喀拉扎组上部的杂基支撑的砾岩具有层状的特点(关旭同等, 2020; Guan *et al.*, 2022, 2023)，分别为泥石流沉积(Nemec and Steel, 1984)和片流沉积(Blair and McPherson, 1994)。

4 准噶尔盆地南缘晚侏罗世风成—冲积沉积体系

在准噶尔盆地南缘的不同剖面，侏罗系—白垩系不整合面上下的沉积环境不同(图 2)。在玛纳斯剖面，上侏罗统喀拉扎组冲积扇砾岩与下白垩统清水河组湖相细粒沉积呈不整合接触(图 9; Fang *et al.*, 2016; Jolivet *et al.*, 2017; Morin *et al.*, 2018; Guan *et al.*, 2024)；在建功煤矿剖面，喀拉扎组风成沉积厚约十余米，与辫状河沉积互层(图 5-c)，上覆清水河组底部为厚层叠置辫状河沉积，向上变为扇三角洲砂砾岩、滨湖相砾岩和湖相细粒沉积(关旭同等, 2020; Guan *et al.*, 2022)；在阿德岗剖面，喀拉扎组风成砂岩与清水河组辫状河砾岩不整合接触；在头屯河剖面以东(图 3)，喀拉扎组风成砂岩与清水河组湖相细粒沉积不整合接触。风成沉积在王家沟剖面厚度最大，



a—喀拉扎组辫状河沉积，顶界平直，为风蚀丘间迁移面；b—喀拉扎组辫状河水成小型槽状交错层理；c—清水河组厚层叠置辫状河道沉积；d—齐古组决口扇沉积；e—齐古组顶部曲流河小型槽状交错层理，河流砂经过了风力作用的搬运、分选和磨圆，结构成熟度高，与风成砂类似；f—齐古组下部曲流河小型槽状交错层理，河流砂岩为红色岩屑杂砂岩，分选、磨圆差

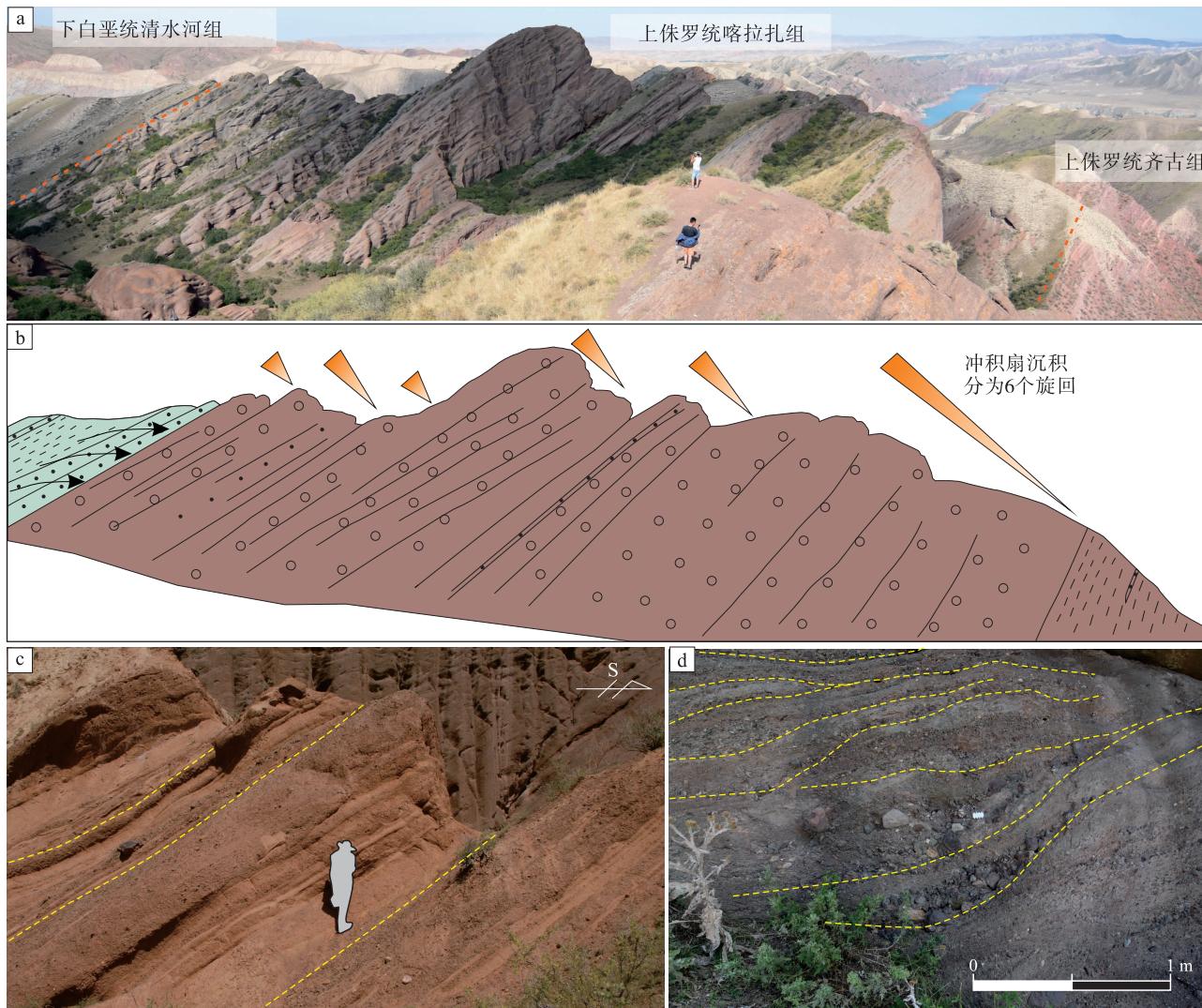
图 8 准噶尔盆地南缘建功煤矿剖面上侏罗统齐古组、喀拉扎组和下白垩统清水河组河流沉积

Fig. 8 River deposits of the Upper Jurassic Qigu and Kalazha Formations and Lower Cretaceous Qingshuihe Formation in Jianguong mine section of southern margin of Junggar Basin

可达约 250 m，向西在建功煤矿剖面、向东在大红山剖面残留沉积厚度减薄(图 2)。

准噶尔盆地南缘晚侏罗世的风成沉积、冲积扇和河流沉积构成了典型的风成—冲积沉积体系(图 10-b)。盆地边缘的冲积扇粗粒沉积，随着搬

运过程粒度变细，分选性和磨圆性增加，在开阔地带形成辫状河和曲流河沉积。根据薄片和粒度分析，建功煤矿、王家沟和头屯河剖面的齐古组顶部的曲流河砂岩具有较好的分选和磨圆(图 6-c；图 7-b)，都主要包含跳跃组分，不同于齐古组下部



a、b—喀拉扎组冲积扇沉积可以划分为 6 个旋回，清水河组湖相沉积上覆于冲积扇砾岩之上；c—冲积扇片流沉积；d—冲积扇河道沉积
图 9 准噶尔盆地南缘玛纳斯剖面喀拉扎组冲积扇砾岩沉积

Fig. 9 Alluvial conglomerates of the Kalazha Formation in Manas section of southern margin of Junggar Basin

典型的由滚动和跳跃组分组成的曲流河砂岩，而类似于风成砂岩(图 7-a)，这说明河流砂经过了风力作用的搬运、分选和磨圆，结构成熟度增加。这一点也被 Guan 等 (2024) 通过碎屑锆石年代学研究所证明，在王家沟—头屯河地区风成沙和河流沙沉积物源相似，古风向与河流古流向正交，说明风成沉积的物质来源于盆地内邻近的河流物质，风成沙也被风搬运到河流沉积中。

准噶尔盆地风成—冲积沉积体系受到晚侏罗世气候干旱化和天山构造活化的共同作用控制。一方面，气候干旱导致沉积物供给减少。基准面上升，头屯河组下部的辫状河沉积演化为头屯河组上部

齐古组的曲流河沉积 (谭程鹏等, 2014; Guan *et al.*, 2024)。Jolivet 等 (2017) 认为喀拉扎组的冲积扇砾岩很大程度上是在干旱气候下由偶发的大型降雨引发的山洪、泥石流造成，因为该冲积扇砾岩由片流和泥石流沉积组成，且在发育风成沉积、少植被的环境下容易发生风化侵蚀并在大型降雨事件中形成粗粒沉积 (Moumani *et al.*, 2003; Davies and Gibling, 2010)。另一方面，风成—冲积沉积体系受到天山构造活化的影响。磷灰石裂变径迹数据表明北天山晚侏罗世和早白垩世发生了构造隆升 (郭召杰等, 2006; 张志诚等, 2007; Jolivet *et al.*, 2010; Tang *et al.*, 2015; Zhang *et al.*,

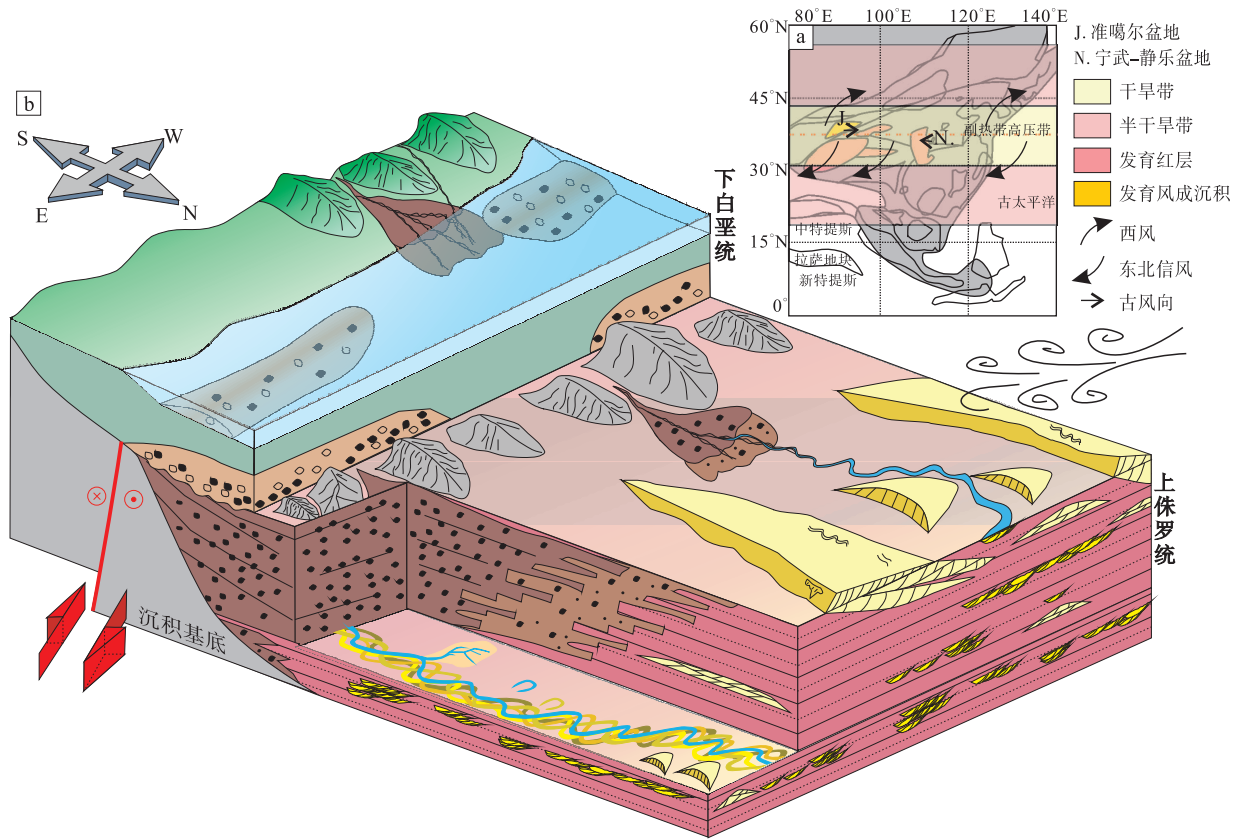


图 10 中亚地区大气环流模型 (a) 下的准噶尔盆地南缘晚侏罗世风成—冲积沉积体系 (b)

Fig. 10 Late Jurassic eolian-alluvial sedimentary system of southern margin of Junggar Basin (b)

under the atmospheric circulation model of Central Asia (a)

2022), 这导致了基准面下降, 形成了风成—沉积体系 (Fang *et al.*, 2016; 张弛等, 2021; Guan *et al.*, 2022, 2024), 风成沉积的范围扩大至东西向 100 km (Guan *et al.*, 2024)。根据磷灰石裂变径迹热史模拟, 头屯河地区未发生构造剥露, 而玛纳斯地区发生了构造剥露 (Zhang *et al.*, 2022), 这可能造成了冲积扇只发育在玛纳斯及邻近地区的沉积格局。与新生代相比, 西天山的总体剥露速率较低 (Jolivet *et al.*, 2010; Zhang *et al.*, 2022)。玛纳斯地区对应的西天山地区构造隆升有利于形成雨影效应, 增加形成冲积扇的山洪数量和强度。

5 对中亚晚侏罗世古环境和古气候的启示

准噶尔盆地晚侏罗世的风成沉积范围可能仅限于盆地南部。在盆地南缘风成沉积的残余沉积范围东西向可达 100 km (图 1; 图 2), 而盆地中部同时期发育湖泊和三角洲沉积 (Fang *et al.*, 2016;

于景维等, 2016)。因为风成沉积中保存了大量沉积物, 所以风成沉积过程减缓了沉积通量信号向湖泊的传递, 从而改变了晚侏罗世的源汇系统 (Bullard and Livingstone, 2002)。

准噶尔盆地南缘的沉积环境在侏罗纪至早白垩世发生的 2 次重要变化记录了中亚地区的气候变化。早侏罗世至中侏罗世早期为沼泽遍布的河流—三角洲沉积体系, 从中侏罗世晚期开始随着气候干旱化演变为风成—冲积沉积体系; 在经历了晚侏罗世天山构造运动后, 准噶尔盆地进入早白垩世拗陷盆地阶段, 气候半干旱半湿润, 湖盆范围扩大, 整体上发育湖泊—三角洲沉积体系。准噶尔盆地的气候变化是东亚区域性气候变化的一部分, 可能与古地理位置变化有关 (Yi *et al.*, 2019)。一次显著的侏罗纪真极移事件 (Torsvik *et al.*, 2012; Kent *et al.*, 2015) 影响了全球所有板块的运动过程。最新的基于燕山造山带的古地磁研究表明, 在 160~145 Ma 发生了快速真极移, 在早白垩世紧接

着发生了第 2 段返程式真极移 (Yi *et al.*, 2019; Hou *et al.*, 2024)。受到真极移事件的影响, 准噶尔盆地的古地理位置从晚三叠世至早侏罗世的 $\sim 71^\circ\text{N}$ 变为晚侏罗世的 $\sim 32^\circ\text{N}$ (Chen *et al.*, 1991; Sha *et al.*, 2015; Olsen *et al.*, 2022, 2024), 从高纬度的湿润带变化到了中纬度干旱带; 在早白垩世古地理位置北移 (Yi *et al.*, 2019), 可能造成了准噶尔盆地发生气候湿润化。此外早白垩世的古气候可能与天山造山带的水汽阻隔有关系 (戴霜等, 2013)。如吐哈盆地、塔里木盆地在早白垩世比准噶尔盆地气候干旱, 吐哈盆地发育石膏沉积和风成沉积 (Zhang *et al.*, 2025), 塔里木盆地发育钙质结核和风成沉积 (陈荣林等, 1994; 梅冥相等, 2004; Jolivet *et al.*, 2018)。这一猜想还需要通过古天山地貌、构造—气候相互作用方面的研究来验证。类似的天山水汽阻隔效应在新生代研究中已被证实, 地质证据和气候模拟共同表明天山阻挡了西风带来的湿润水汽并造成了中亚干旱和天山周缘盆地气候分异 (Wang *et al.*, 2020)。

东亚、中亚地区的晚侏罗世—白垩纪存在多处风成沉积, 根据恢复得到的古风向, 认为古风向受控于行星风系 (图 10-a; 许欢等, 2013; Qiao *et al.*, 2022; Cao *et al.*, 2023; Wang *et al.*, 2024; Zhang *et al.*, 2025)。根据塔里木、吐哈、柴达木等盆地的下白垩统风成沉积古风向 (江新胜等, 2009; 胡俊杰等, 2018; 陈政宇等, 2020; Zhang *et al.*, 2025), Zhang 等 (2025) 推断中亚地区在早白垩世主要处于西风带。通过测量准噶尔盆地南缘晚侏罗世风成沉积的大型高角度交错层理的产状并校正得到的古风向为自西向东 (图 2)。邻近的吐哈盆地在早白垩世的贝里阿斯期至瓦兰今期处于西风带, 推测准噶尔盆地晚侏罗世风成沉积形成于西风带。而宁武—静乐盆地的晚侏罗世风成沉积的古风向主要为自东向西 (Xu *et al.*, 2019), 因此推测副热带高压带在晚侏罗世处于这 2 个盆地之间 (图 10-a)。在早白垩世的贝里阿斯期至瓦兰今期, 吐哈盆地和华北地区的古风向为自西向东, 鄂尔多斯盆地的古风向为交替的西风 and 东风, 因此推测副热带高压带处于鄂尔多斯盆地附近; 在早白垩世的欧特里夫期晚期至巴雷姆期, 鄂尔多斯盆地和塔里木盆地西南缘分别具有自西向东和自东向西的古风向,

因此推测副热带高压带在晚侏罗世处于这 2 个盆地之间 (Zhang *et al.*, 2025)。综上, 副热带高压带自晚侏罗世至早白垩世逐渐南移。但值得注意的是, 该推断是基于行星风系模型 (图 10-a), 且局部的古地理或古地貌可能导致局部风成砂发育以及古风向变化 (Wu *et al.*, 2024), 因此关于中生代大气环流和古地貌对大气环流的影响还需要进一步研究。

6 结论

通过分析准噶尔盆地南缘晚侏罗世沉积环境, 得到以下结论:

1) 准噶尔盆地南缘晚侏罗世古沙地位于侏罗系—白垩系不整合面之下, 古风成沙地残留沉积范围东西向可达 100 km。在王家沟剖面沉积厚度最厚, 约 250 m; 沉积厚度向西减薄, 在建功煤矿剖面的风成沉积砂体厚度约十余米, 且受到多期砾质辫状河的冲刷。

2) 准噶尔盆地晚侏罗世古风成沙地的沉积物来源于附近河流沙, 风成沙又为河流沉积提供物源。风成和河流沉积交互出现, 且河流沙和同期的风成沙具有相似的粒度组成和沉积物源。此外, 古风向与河流古流向正交的沉积格局有利于风成和河流沉积的物质交换。这些都说明了风成沉积和河流沉积的密切关系。

3) 晚侏罗世风成—冲积沉积体系受到气候干旱化和天山构造活动的控制, 气候干旱导致沉积物供给减少, 沉积基准面上升, 头屯河组下部的辫状河沉积演变为头屯组上部和齐古组的季节性曲流河; 天山的构造活化导致沉积基准面下降, 在准噶尔盆地南缘风成沉积范围扩大, 冲积扇沉积广泛分布。

4) 准噶尔盆地南缘自侏罗纪至早白垩世经历的 2 次重要的沉积格局变化记录了中亚内陆地区的气候变化。在中侏罗世晚期气候干旱化的影响下, 河流—三角洲体系变化到风成—冲积沉积体系; 在早白垩世气候湿润化的影响下, 沉积体系转变为湖泊—三角洲沉积体系。

致谢 感谢审稿人柳永清研究员和张昌民教授宝贵的意见! 审稿意见对于提升此文起到了重要作用。感谢林聪博士在野外工作中的协助!

参考文献 (References)

- 陈荣林,朱宏发,徐良发. 1994. 塔里木盆地西南拗陷下白垩统风成砂岩的发现及其意义. 科学通报,39(1): 58-60. [Chen R L, Zhu H F, Xu L F. 1994. Discovery and significance of aeolian ore-bearing rocks in the Lower Cretaceous of the southwestern depression, Tarim Basin. Chinese Science Bulletin, 39(1): 58-60]
- 陈政宇,柳永清,江小均,孔志岗,高万里,钱涛,旷红伟,许欢. 2020. 柴达木旺尕秀煤矿东南晚侏罗世一早白垩世风成砂古风向及古地理意义. 地学前缘,27(4): 82-97. [Chen Z Y, Liu Y Q, Jiang X J, Kong Z G, Gao W L, Qian T, Kuang H W, Xu H. 2020. Paleowind direction and paleogeographic significance of Late Jurassic to Early Cretaceous anemoarenite in the southeastern Wanggaxiu coal mine, Qaidam Basin. Earth Science Frontiers, 27(4): 82-97]
- 戴霜,张明震,彭栋祥,王华伟,吴茂先,陈瑞灵. 2013. 中国西北地区中—新生代构造与气候格局演化. 海洋地质与第四纪地质, 33(4): 153-168. [Dai S, Zhang M Z, Peng D X, Wang H W, Wu M X, Chen R L. 2013. The Mesozoic-Cenozoic evolution of the tectonic and climatic patterns, NW China. Marine Geology & Quaternary Geology, 33(4): 153-168]
- 邓胜徽,王思恩,杨振宇,卢远征,李鑫,胡清月,安纯志,席党鹏,万晓樵. 2015. 新疆准噶尔盆地中、晚侏罗世多重地层研究. 地球学报, 36(5): 559-574. [Deng S H, Wang S S, Yang Z Y, Lu Y Z, Li X, Hu Q Y, An C Z, Xi D P, Wan X Q. 2015. Comprehensive study of the Middle-Upper Jurassic strata in the Junggar Basin, Xinjiang. Acta Geoscientica Sinica, 36(5): 559-574]
- 方世虎,贾承造,郭召杰,宋岩,徐怀民,刘楼军. 2006. 准噶尔盆地二叠纪盆地属性的再认识及其构造意义. 地学前缘, 13(3): 108-121. [Fang S H, Jia C Z, Guo Z J, Song Y, Xu H M, Liu L J. 2006. New view on the Permian evolution of the Junggar Basin and its implications for tectonic evolution. Earth Science Frontiers, 13(3): 108-121]
- 高志勇,周川闽,冯佳睿,崔京钢,郭美丽,吴昊. 2015. 盆地内大面积砂体分布的一种成因机理: 干旱气候下季节性河流沉积. 沉积学报, 33(3): 427-438. [Gao Z Y, Zhou C M, Feng J R, Cui J G, Guo M L, Wu H. 2015. Distribution of a large area of sand body formation mechanism: ephemeral streams in arid climate. Acta Sedimentologica Sinica, 33(3): 427-438]
- 关旭同,吴鉴,魏凌云,赵进雍,冯庚,李严. 2019. 准噶尔盆地南缘建功煤矿剖面齐古组河流沉积与砂体构型. 新疆石油地质, 40(3): 290-297. [Guan X T, Wu J, Wei L Y, Zhao J Y, Feng G, Li Y. 2019. Meandering river deposit and sand body architecture in Qigu Formation of Jiangong coal mine section in the southern margin of Junggar Basin. Xinjiang Petroleum Geology, 40(3): 290-297]
- 关旭同,吴朝东,吴鉴,周家全,焦悦,周嵘,于庆森. 2020. 准噶尔盆地南缘上侏罗统—下白垩统沉积序列及沉积环境演化. 新疆石油地质, 41(1): 67-79. [Guan X T, Wu C D, Wu J, Zhou J Q, Jiao Y, Zhou R, Yu Q S. 2020. Sedimentary sequence and depositional environment evolution of Upper Jurassic-Lower Cretaceous strata in the southern margin of Junggar Basin. Xinjiang Petroleum Geology, 41(1): 67-79]
- 郭召杰,张志诚,吴朝东,方世虎,张锐. 2006. 中、新生代天山隆升过程及其与准噶尔、阿尔泰山比较研究. 地质学报, 80(1): 1-15. [Guo Z J, Zhang Z C, Wu C D, Fang S H, Zhang R. 2006. The Mesozoic and Cenozoic exhumation history of Tianshan and comparative studies to the Junggar and Altai Mountains. Acta Geologica Sinica, 80(1): 1-15]
- 何登发,张磊,吴松涛,李涤,甄宇. 2018. 准噶尔盆地构造演化阶段及其特征. 石油与天然气地质, 39(5): 845-861. [He D F, Zhang L, Wu S T, Li D, Zhen Y. 2018. Tectonic evolution stages and features of the Junggar Basin. Oil & Gas Geology, 39(5): 845-861]
- 胡俊杰,马寅生,吴祎,王宗秀,柳永清,高万里,李宗星,魏小洁. 2018. 柴达木盆地旺尕秀地区上侏罗统一早白垩统风成砂的发现及其意义. 古地理学报, 20(5): 776-786. [Hu J J, Ma Y S, Wu Y, Wang Z X, Liu Y Q, Gao W L, Li Z X, Wei X J. 2018. Discovery and significance of the Upper Jurassic-Lower Cretaceous eolian sands in Wanggaxiu area, Qaidam Basin. Journal of Palaeogeography (Chinese Edition), 20(5): 776-786]
- 江新胜,蔡习尧,潘忠习,熊国庆,伍皓. 2009. 塔里木盆地西南部早白垩统风成沙丘古风向测量与古风带恢复. 沉积与特提斯地质, 29(4): 1-4. [Jiang X S, Cai X Y, Pan Z X, Xiong G Q, Wu H. 2009. Palaeowind direction measurements and palaeowind belt reconstruction of the Early Cretaceous eolian dunes in southwestern Tarim Basin, Xinjiang. Sedimentary Geology and Tethyan Geology, 29(4): 1-4]
- 李孝泽,董光荣,靳鹤龄,苏志珠,王远平. 1999. 鄂尔多斯白垩系沙丘岩的发现. 科学通报, 44(8): 874-878. [Li X Z, Dong G R, Jin H L, Su Z Z, Wang Y P. 1999. Discovery of Cretaceous aeolian sandstone in the Ordos Basin. Chinese Science Bulletin, 44(8): 874-878]
- 梁则亮,庞志超,冀冬生,冯兴强,吴林,施辉. 2020. 四棵树凹陷超深层裂谷盆地的厘定及油气勘探意义. 新疆石油地质, 41(1): 18-24. [Liang Z L, Pang Z C, Ji D S, Feng X Q, Wu L, Shi H. 2020. Discovery of ultra-deep rift basin and its petroleum exploration significance in Sikeshu sag, Junggar Basin. Xinjiang Petroleum Geology, 41(1): 18-24]
- 梅冥相,苏德辰. 2014a. 甘肃张掖地区白垩系风成砂岩沉积序列: 祁连山白垩纪隆升的沉积学响应. 古地理学报, 16(2): 143-156. [Mei M X, Su D C. 2014a. Cretaceous sedimentary succession of eolian sandstones in Zhangye Region of Gansu Province: sedimentological response to the Cretaceous uplift of Qilian Mountains. Journal of Palaeogeography (Chinese Edition), 16(2): 143-156]
- 梅冥相,苏德辰. 2014b. 甘肃古浪河口群粗碎屑岩系的层序地层序列: 祁连山白垩纪隆升的沉积学响应. 地质论评, 60(3): 541-554. [Mei M X, Su D C. 2014b. Sequence-stratigraphic succession for the course clastic rock system of the Hekou Group in the Gulang County of Gansu Province: sedimentological response to the Cretaceous uplift of the Qilian Mountains. Geological Review, 60(3): 541-554]
- 梅冥相,于炳松,靳卫广. 2004. 塔里木盆地北缘库车盆地白垩系风成砂岩研究; 以库车河剖面为例. 地质通报, 23(12): 1221-1227. [Mei M X, Yu B S, Jin W G. 2004. Cretaceous eolian sand-

- stones in the Kuqa basin on the northern margin of the Tarim Basin: a case study of the Kuqa River section. *Geological Bulletin of China*, 23(12): 1221–1227]
- Schneider W, 赵霞飞, 龙能礼, 赵永胜, Martin F. 1992. 准噶尔盆地头屯河地区侏罗系沉积环境与构造意义. *新疆石油地质*, 10(3): 191–202. [Schneider W, Zhao X F, Long N L, Zhao Y S, Martin F. 1992. Sedimentary environment and tectonic implication of Jurassic in Toutunhe area, Junggar Basin. *Xinjiang Petroleum Geology*, 10(3): 191–202]
- 司学强, 袁波, 彭博, 冀冬生, 郭华军, 唐雪颖, 窦洋, 李亚哲. 2021. 准噶尔盆地南缘冲断带侏罗系喀拉扎组沉积特征. *新疆石油地质*, 42(4): 389–398. [Si X Q, Yuan B, Peng B, Ji D S, Guo H J, Tang X Y, Dou Y, Li Y Z. 2021. Sedimentary characteristics of Jurassic Kalazha Formation in the thrust belt on the southern margin of Junggar Basin. *Xinjiang Petroleum Geology*, 42(4): 389–398]
- 谭程鹏, 于兴河, 李胜利, 李顺利, 陈彬滔, 单新, 王志兴. 2014. 辫状河一曲流河转换模式探讨: 以准噶尔盆地南缘头屯河组露头为例. *沉积学报*, 32(3): 450–458. [Tan C P, Yu X H, Li S L, Li S L, Chen B T, Shan X, Wang Z X. 2014. Discussion on the model of braided river transform to meandering river: as an example of Toutunhe Formation in Southern Junggar Basin. *Acta Sedimentologica Sinica*, 32(3): 450–458]
- 田业. 2017. 准噶尔盆地中西部地区侏罗纪孢粉组合及古气候研究. 中国地质大学(北京)硕士学位论文. [Tian Y. 2017. Study on Jurassic palynological assemblages and paleoclimate of the mid-western area of the Junggar Basin. Masteral dissertation of China University of Geosciences(Beijing)]
- 王长轩. 2014. 新疆车排子地区孢粉植物群与古气候. *微体古生物学报*, 31(1): 75–84. [Wang C X. 2014. Spore-pollen flora and paleoclimate of the Chepaizi area, Xinjiang, NW China. *Acta Micro-palaeontologica Sinica*, 31(1): 75–84]
- 新疆维吾尔自治区地质矿产局. 1999. 新疆维吾尔自治区岩石地层. 武汉: 中国地质大学出版社. [Geological and Mineral Bureau of the Xinjiang Uygur Autonomous Region. 1999. Lithostratigraphy of the Xinjiang Uygur Autonomous Region. Wuhan: China University of Geosciences Press]
- 许欢, 柳永清, 旷红伟, 刘燕青, 彭楠, 董超, 薛沛霖, 徐加林, 陈军, 刘海. 2013. 华北晚侏罗世—早白垩世风成砂沉积及其古地理和古生态学意义. *古地理学报*, 15(1): 11–30. [Xu H, Liu Y Q, Kuang H W, Liu Y X, Peng N, Dong C, Xue P L, Xu J L, Chen J, Liu H. 2013. Sedimentology, palaeogeography and palaeoecology of the Late Jurassic-Early Cretaceous eolian sands in North China. *Journal of Palaeogeography (Chinese Edition)*, 15(1): 11–30]
- 于景维, 柳妮, 文华国, 朱永才, 张宗斌. 2016. 准噶尔盆地阜东斜坡区上侏罗统齐古组高分辨率层序分析及砂体预测. *古地理学报*, 18(2): 265–274. [Yu J W, Liu N, Wen H G, Zhu Y C, Zhang Z B. 2016. Analysis of high-resolution sequence stratigraphy and prediction of favorable sandbodies in the Upper Jurassic Qigu Formation in Fudong slope area, Junggar Basin. *Journal of Palaeogeography (Chinese Edition)*, 18(2): 265–274]
- 张昌民, 付文俊, 冀东升, 赵康, 张祥辉. 2023. 准噶尔盆地南缘上侏罗统喀拉扎组沉积储层研究进展. *长江大学学报(自然科学版)*, 20(1): 1–14. [Zhang C M, Fu W J, Ji D S, Zhao K, Zhang X H. 2023. Research progress on the sedimentary reservoirs of the Upper Jurassic Karaza Formation on the southern margin of the Junggar Basin. *Journal of Yangtze University (Natural Science Edition)*, 20(1): 1–14]
- 张朝军, 何登发, 吴晓智, 石昕, 罗建宁, 王宝瑜, 杨庚, 管树巍, 赵霞. 2006. 准噶尔多旋回叠合盆地的形成与演化. *中国石油勘探*, 11(1): 47–58. [Zhang C J, He D F, Wu X Z, Shi X, Luo J N, Wang B Y, Yang G, Guan S W, Zhao X. 2006. Formation and evolution of multicycle superimposed basins in Junggar Basin. *China Petroleum Exploration*, 11(1): 47–58]
- 张驰, 于兴河, 姚宗全, 李顺利, 单新, 向曼, 李亚龙. 2021. 准噶尔盆地南缘西段中、上侏罗统沉积演化及控制因素分析. *中国地质*, 48(1): 284–296. [Zhang C, Yu X H, Yao Z Q, Li S L, Shan X, Xiang M, Li Y L. 2021. Sedimentary evolution and controlling factors of the Middle–Upper Jurassic in the western part of the southern Junggar Basin. *Geology in China*, 48(1): 284–296]
- 张志诚, 郭召杰, 吴朝东, 方世虎. 2007. 天山北缘侏罗系地层热历史演化及其地质意义: 磷灰石裂变径迹和镜质体反射率证据. *岩石学报*, 23(7): 1683–1695. [Zhang Z C, Guo Z J, Wu C D, Fang S H. 2007. Thermal history of the Jurassic strata in the northern Tianshan and its geological significance, revealed by apatite fission-track and vitrinite-reflectance analysis. *Acta Petrologica Sinica*, 23(7): 1683–1695]
- 周天琪, 吴朝东, 袁波, 史忠奎, 王家林, 朱文, 周彦希, 姜晰, 赵进雍, 王军, 马健. 2019. 准噶尔盆地南缘侏罗系重矿物特征及其物源指示意义. *石油勘探与开发*, 46(1): 65–78. [Zhou T Q, Wu C D, Yuan B, Shi Z K, Wang J L, Zhu W, Zhou Y X, Jiang X, Zhao J Y, Wang J, Ma J. 2019. New insights into multiple provenances evolution of the Jurassic from heavy minerals characteristics in southern Junggar Basin, NW China. *Petroleum Exploration and Development*, 46(1): 65–78]
- Allen J R. 1965. A review of the origin and characteristics of recent alluvial sediments. *Sedimentology*, 5: 89–191.
- Ashraf A R, Sun Y, Sun G, Uhl D, Mosbrugger V, Li J, Herrmann M. 2010. Triassic and Jurassic palaeoclimate development in the Junggar Basin, Xinjiang, Northwest China: a review and additional lithological data. *Palaeobiodiversity and Palaeoenvironments*, 90: 187–201.
- Blair T C, McPherson J G. 1994. Alluvial fans and their natural distinction from rivers based on morphology, hydraulic processes, sedimentary processes, and facies assemblages. *Journal of Sedimentary Research*, 64: 450–489.
- Buatois L A, Mángano M G. 2004. Ichnology of fluvio-lacustrine environments: animal-substrate interactions in freshwater ecosystems. In: McIlroy D (ed). *The application of ichnology to palaeoenvironmental and stratigraphic analysis*. Geological Society of London, Special Publication, 228: 311–333.
- Bullard J E, Livingstone I. 2002. Interactions between aeolian and fluvial systems in dryland environments. *Area*, 34: 8–16.
- Cao S, Ma J, Wang C. 2023. The sedimentological characteristics of the intermontane desert system in the Jurong Basin, South China, and its relationship with the Late Cretaceous hot climate. *Palaeogeography*,

- Palaeoclimatology, Palaeoecology, 623: 111618.
- Chen Y, Cogne J P, Courtillot V, Avouac J P, Tapponnier P, Wang G, Bai M, You H, Li M, Wei C, Buffetaut E. 1991. Paleomagnetic study of Mesozoic continental sediments along the northern Tien Shan (China) and heterogeneous strain in central Asia. *Journal of Geophysical Research: Solid Earth*, 96: 4065–4082.
- Chesley J T, Leier A L, White S, Torres R. 2017. Using unmanned aerial vehicles and structure-from-motion photogrammetry to characterize sedimentary outcrops: an example from the Morrison formation, Utah, USA. *Sedimentary Geology*, 354: 1–8.
- Clemmensen L B, Abrahamsen K. 1983. Aeolian stratification and facies association in desert sediments, Arran Basin (Permian), Scotland. *Sedimentology*, 30: 311–339.
- Davies N S, Gibling M R. 2010. Cambrian to Devonian evolution of alluvial systems: the sedimentological impact of the earliest land plants. *Earth-Science Reviews*, 98: 171–200.
- Eberth D A, Brinkman D B, Chen P, Yuan F, Wu S, Li G, Cheng X. 2001. Sequence stratigraphy, paleoclimate patterns, and vertebrate fossil preservation in Jurassic and Cretaceous strata of the Junggar Basin, Xinjiang Autonomous Region, People's Republic of China. *Canadian Journal of Earth Sciences*, 38: 1627–1644.
- Elberhiti H, Andreotti B, Claudin P. 2008. Barchan dune corridors: field characterization and investigation of control parameters. *Journal of Geophysical Research: Earth Surface*, 113: F2.
- Fang Y, Wu C, Wang Y, Wang L, Guo Z, Hu H. 2016. Stratigraphic and sedimentary characteristics of the Upper Jurassic-Lower Cretaceous strata in the Junggar Basin, Central Asia: tectonic and climate implications. *Journal of Asian Earth Sciences*, 129: 294–308.
- Frey R W, Pemberton S G, Fagerstrom J A. 1984. Morphological, ethological and environmental significance of the ichnogenera *Scoyenia* and *Ancorichnus*. *Journal of Paleontology*, 58: 511–528.
- Fryberger S G, Ahlbrandt T S, Andrews S. 1979. Origin, sedimentary features, and significance of low-angle eolian “sand sheet” deposits, Great Sand Dunes National Monument and vicinity, Colorado. *Journal of Sedimentary Research*, 49: 733–746.
- Gao Z, Shi Y, Feng J, Zhou C, Luo Z. 2022. Lithofacies paleogeography restoration and its significance of Jurassic to Lower Cretaceous in southern margin of Junggar Basin, NW China. *Petroleum Exploration and Development*, 49: 78–93.
- Guan S, Stockmeyer J M, Shaw J H, Plesch A, Zhang J. 2016. Structural inversion, imbricate wedging, and out-of-sequence thrusting in the southern Junggar fold-and-thrust belt, northern Tien Shan, China. *AAPG Bulletin*, 100: 1443–1468.
- Guan X, Wu C, Zhou T, Tang X, Ma J, Fang Y. 2021. Jurassic-Lower Cretaceous sequence stratigraphy and allogenic controls in proximal terrestrial environments (Southern Junggar Basin, NW China). *Geological Journal*, 56: 4038–4062.
- Guan X, Wu C, Zhang X, Jia W, Zhang W. 2022. Sedimentary and source-to-sink evolution of intracontinental basins: implications for tectonic and climate evolution in the late Mesozoic (Southern Junggar Basin, NW China). *Frontiers in Earth Science*, 9: 785659.
- Guan X, Wu C, Wang B, Zhou T, Xu Y, Tang X, Xie L. 2023. Sediment provenances of a Mesozoic intracontinental basin enclosed by multiple orogenic belts, Junggar Basin, NW China: insights from detrital ilmenite, Cr-spinel geochemistry, and zircon U-Pb geochronology. *International Geology Review*, 65: 2067–2092.
- Guan X, Wu C, Xu Y, Jolivet M, Xiu J, Lin C. 2024. A fluvial-aeolian system in response to aridification during the Late Mesozoic, Junggar Basin, Central Asia. *Basin Research*, 36: e12879.
- Hein F J, Walker R G. 1977. Bar evolution and development of stratification in the gravelly, braided, Kicking Horse River, British Columbia. *Canadian Journal of Earth Sciences*, 14: 562–570.
- Hou Y, Zhao P, Qin H, Mitchell R N, Li Q, Hao W, Zhang M, Ward P, Yuan J, Deng C, Zhu R. 2024. Completing the loop of the Late Jurassic–Early Cretaceous true polar wander event. *Nature Communications*, 15: 2183.
- Hunter R E. 1977. Basic types of stratification in small eolian dunes. *Sedimentology*, 24: 361–387.
- Jolivet M, Dominguez S, Charreau J, Chen Y, Li Y, Wang Q. 2010. Mesozoic and Cenozoic tectonic history of the central Chinese Tian Shan: reactivated tectonic structures and active deformation. *Tectonics*, 29: TC6019.
- Jolivet M, Bourquin S, Heilbronn G, Robin C, Barrier L, Dabard M, Jia Y, De Pelsmaecker E, Fu B. 2017. The Upper Jurassic-Lower Cretaceous alluvial-fan deposits of the Kalaza Formation (Central Asia): tectonic pulse or increased aridity? *Geological Society, London, Special Publications*, 427: 491–521.
- Jolivet M, Boulvais P, Barrier L, Robin C, Heilbronn G, Ledoyen J, Ventoux Q, Jia Y, Guo Z, Bataleva E A. 2018. Oxygen and carbon stable isotope composition of Cretaceous to Pliocene calcareous paleosols in the Tian Shan Region (Central Asia): controlling factors and paleogeographic implications. *Geosciences*, 8: 330.
- Kent D V, Kjarsgaard B A, Gee J S, Muttoni G, Heaman L M. 2015. Tracking the Late Jurassic apparent (or true) polar shift in U-Pb-dated kimberlites from cratonic North America (Superior Province of Canada). *Geochemistry, Geophysics, Geosystems*, 16: 983–994.
- Kocurek G. 1991. Interpretation of ancient eolian sand dunes. *Annual Review of Earth and Planetary Sciences*, 19: 43–75.
- Kocurek G, Dott Jr. R H. 1981. Distinction and uses of stratification types in the interpretation of eolian sand. *Journal of Sedimentary Petrology*, 51: 579–595.
- Langford R P, Chan M A. 1989. Fluvial-eolian interactions: part II, ancient systems. *Sedimentology*, 36: 1037–1051.
- Morin J, Jolivet M, Robin C, Heilbronn G, Barrier L, Bourquin S, Jia Y. 2018. Jurassic paleogeography of the Tian Shan: an evolution driven by far-field tectonics and climate. *Earth-Science Reviews*, 187: 286–313.
- Moumani K, Alexander J, Bateman M D. 2003. Sedimentology of the Late Quaternary Wadi Hasa Marl Formation of Central Jordan: a record of climate variability. *Palaeogeography, Palaeoclimatology, Palaeoecology*, 191: 221–241.
- Mountney N P. 2006. Eolian facies models. In: Posamentier H W, Walker R G (eds). *Facies Model Revised*. SEPM Special Publication, 19–83.
- Nemec W, Steel R J. 1984. Alluvial and coastal conglomerates: their significant features and some comments on gravelly-massflow deposits.

- In: Koster E H, Steel R J (eds). *Sedimentology of Gravels and Conglomerates*. Canadian Society of Petroleum Geologists, 10: 1–31.
- Nieminski N M, Graham S A. 2017. Modeling stratigraphic architecture using small unmanned aerial vehicles and photogrammetry: examples from the Miocene East Coast Basin, New Zealand. *Journal of Sedimentary Research*, 87: 126–132.
- Olsen P E, Sha J, Fang Y, Chang C, Whiteside J H, Kinney S, Sues H, Kent D, Schaller M, Vajda V. 2022. Arctic ice and the ecological rise of the dinosaurs. *Science Advances*, 8: eabo6342.
- Olsen P E, Sha J, Fang Y, Chang C, Kent D V, Vajda V, Whiteside J H, Kinney S, Lampert A, MacLennan S A. 2024. Empirical record, geochronology and theoretical determinates of Mesozoic climate in the Junggar Basin, NW China, in relation to other basins in NE China. Geological Society, London, Special Publications, 538: 235–260.
- Peng Z, Wang X, Graveleau F, Vendeville B C, Nunns A G. 2024. Structural interactions between deep Mesozoic strike-slip faults and shallow Cenozoic contractional folds in the Northern Tianshan Foreland Basin (NW China). *Tectonics*, 43: e2023TC007986.
- Qiao D, Peng N, Kuang H, Liu Y, Liu Y, Cui L, Wang Y. 2022. Changes in prevailing surface-paleowinds reveal the atmospheric circulation transition during Early Cretaceous in North China. *Palaeogeography, Palaeoclimatology, Palaeoecology*, 586: 110784.
- Rodríguez-López J P, Melendez N, De Boer P L, Soria A R. 2008. Aeolian sand sea development along the mid-Cretaceous western Tethyan margin (Spain): erg sedimentology and palaeoclimate implications. *Sedimentology*, 55: 1253–1292.
- Scotese C R. 2016. Paleomap paleoatlas for GPlates and the paleodata plotter program: PALEOMAP project. [Online] Available at: <https://www.earthbyte.org/paleomap-paleoatlas-for-gplates/> (Accessed August 2024).
- Sha J, Olsen P E, Pan Y, Xu D, Wang Y, Zhang X, Yao X, Vivi V. 2015. Triassic-Jurassic climate in continental high-latitude Asia was dominated by obliquity-paced variations Junggar Basin, Ürtimqi, China. *Proceedings of the National Academy of Sciences*, 112: 3624–3629.
- Sha J, Fang Y, Cheng J, Wang Y, Li S, Yang X, Li J, Zhang H. 2023. Geologic and chronostratigraphic overview of the Upper Triassic and Jurassic successions of the Junggar Basin, NW China. Geological Society, London, Special Publications, 538: SP538–2022.
- Simplicio F, Basilici G. 2015. Unusual thick eolian sand sheet sedimentary succession: paleoproterozoic Bandeirinha Formation, Minas Gerais. *Brazilian Journal of Geology*, 45: 3–11.
- Tang W, Zhang Z, Li J, Li K, Luo Z, Chen Y. 2015. Mesozoic and Cenozoic uplift and exhumation of the Bogda Mountain, NW China: evidence from apatite fission track analysis. *Geoscience Frontiers*, 6: 617–625.
- Torsvik T H, Van der Voo R, Preeden U, Mac Niocaill C, Steinberger B, Doubrovine P V, Hinsbergen D, Domeier M, Gaina C, Tohver E, Meert J, McCausland P, Cocks L. 2012. Phanerozoic polar wander, palaeogeography and dynamics. *Earth-Science Reviews*, 114: 325–368.
- Vincent S J, Allen M B. 2001. Sedimentary record of Mesozoic intracontinental deformation in the eastern Junggar Basin, northwest China: response to orogeny at the Asian margin. *Geological Society of America Memoirs*, 194: 341–360.
- Wang F, Li Z, Sun X, Zhao J, Fan Y, Xia D, Ayyamperumal R, Li B. 2024. Early Cretaceous (Late Barremian–Early Albian) expanding aeolian activity in East Asia: evidence from the stratigraphic evolution of aeolian deposition in the Baiyin–Jingyuan Basin, northern China. *Geological Society of America Bulletin*, 136: 487–512.
- Wang X, Carrapa B, Sun Y, Dettman D L, Chapman J B, Caves Rugenstein J K, Clementz, DeCelles, Wang M, Chen J, Quade, Wang F, Li Z, Oimuhammadzoda I, Gadoev M, Lohmann G, Zhang X, Chen F. 2020. The role of the westerlies and orography in Asian hydroclimate since the late Oligocene. *Geology*, 48: 728–732.
- Wang Y, Mosbrugger V, Zhang H. 2005. Early to Middle Jurassic vegetation and climatic events in the Qaidam Basin, Northwest China. *Palaeogeography, Palaeoclimatology, Palaeoecology*, 224: 200–216.
- Wang Y, Jia D, Pan J, Wei D, Tang Y, Wang G, Wei C, Ma D. 2018. Multiple-phase tectonic superposition and reworking in the Junggar Basin of northwestern China: implications for deep-seated petroleum exploration. *AAPG Bulletin*, 102: 1489–1521.
- Westoby M J, Brasington J, Glasser N F, Hambrey M J, Reynolds J M. 2012. ‘Structure-from-motion’ photogrammetry: a low-cost, effective tool for geoscience applications. *Geomorphology*, 179: 300–314.
- Wu C, Sun X, Li G, Huang L, Jiao H, Li Z, Jian X, Mason C, Rodríguez-López J P. 2024. Cretaceous mountain building processes triggered the aridification and drainage evolution in East Asia. *Geological Society of America Bulletin*, 136: 1863–1877.
- Xie W Q, Wang W H, Tan J Q, Liu Z J, Wang Y, Song X Q, Mansour A. 2024. Late Middle Jurassic aridification event in the Qaidam Basin, Northwest China: palynological and geochemical evidences. *Palaeoworld*, 33: 1044–1064.
- Xu H, Liu Y, Kuang H, Peng N. 2019. Late Jurassic fluvial-eolian deposits from the Tianchihe Formation, Ningwu–Jingle Basin, Shanxi Province, China. *Journal of Asian Earth Sciences*, 174: 245–262.
- Xu X, Clark J M, Eberth D A, Currie P J. 2022. The Shishugou Fauna of the Middle–Late Jurassic transition period in the Junggar Basin of western China. *Acta Geologica Sinica (English Edition)*, 96: 1115–1135.
- Yi Z, Liu Y, Meert J G. 2019. A true polar wander trigger for the Great Jurassic East Asian aridification. *Geology*, 47: 1112–1116.
- Zhang D, Wang G, Pullen A, Abell J T, Cheng F, Shen T, Ji J, Zhang M. 2025. A westerly dominated Early Cretaceous eolian system in the Hami Basin, NW China. *Geological Society of America Bulletin*, 137: 137–155.
- Zhang H, Zhang Z, Tang W, Li K, Li J, Wang Q, Ding C. 2022. Burial and exhumation history of Jurassic sedimentary rocks in the southern margin of the Junggar Basin: implications for the growth of the northern Tianshan Mountains. *Journal of Asian Earth Sciences*, 236: 105339.
- Zhang M, Dai S, Heimhofer U, Wu M, Wang Z, Pan B. 2014. Palynological records from two cores in the Gongpoquan Basin, Central East Asia: evidence for floristic and climatic change during the Late Jurassic to Early Cretaceous. *Review of Palaeobotany and Palynology*, 204: 1–17.